

Cite this: *J. Mater. Chem. B*, 2023, 11, 1389

# Cell-binding peptides on the material surface guide stem cell fate of adhesion, proliferation and differentiation†

Tzu-Cheng Sung,<sup>‡a</sup> Ting Wang,<sup>‡a</sup> Qian Liu,<sup>‡a</sup> Qing-Dong Ling,<sup>b</sup> Suresh Kumar Subbiah,<sup>c</sup> Remya Rajan Renuka,<sup>c</sup> Shih-Tien Hsu,<sup>d</sup> Akihiro Umezawa<sup>e</sup> and Akon Higuchi<sup>‡\*afg</sup>

Human cells, especially stem cells, need to communicate and interact with extracellular matrix (ECM) proteins, which not only serve as structural components but also guide and support cell fate and properties such as cell adhesion, proliferation, survival and differentiation. The binding of the cells with ECM proteins or ECM-derived peptides *via* cell adhesion receptors such as integrins activates several signaling pathways that determine the cell fate, morphological change, proliferation and differentiation. The development of synthetic ECM protein-derived peptides that mimic the biological and biochemical functions of natural ECM proteins will benefit academic and clinical application. Peptides derived from or inspired by specific ECM proteins can act as agonists of each ECM protein receptor. Given that most ECM proteins function in cell adhesion *via* integrin receptors, many peptides have been developed that bind to specific integrin receptors. In this review, we discuss the peptide sequence, immobilization design, reaction method, and functions of several ECM protein-derived peptides. Various peptide sequences derived from mainly ECM proteins, which are used for coating or grafting on dishes, scaffolds, hydrogels, implants or nanofibers, have been developed to improve the adhesion, proliferation or differentiation of stem cells and to culture differentiated cells. This review article will help to inform the optimal choice of ECM protein-derived peptides for the development of scaffolds, implants, hydrogels, nanofibers and 2D cell culture dishes to regulate the proliferation and direct the differentiation of stem cells into specific lineages.

Received 29th November 2022,  
Accepted 30th December 2022

DOI: 10.1039/d2tb02601e

rsc.li/materials-b

<sup>a</sup> State Key Laboratory of Ophthalmology, Optometry and Visual Science, Eye Hospital, Wenzhou Medical University, No. 270, Xueyuan Road, Wenzhou, Zhejiang, 325027, China. E-mail: higuchi@wmu.edu.cn; Fax: +86-577-88824115; Tel: +86-577-88824116

<sup>b</sup> Cathay Medical Research Institute, Cathay General Hospital, No. 32, Ln 160, Jian-Cheng Road, Hsi-Chi City, Taipei 221, Taiwan

<sup>c</sup> Centre for Materials Engineering and Regenerative Medicine, Bharath Institute of Higher Education and Research, 173, Agaram Road, Tambaram East, Chennai-73, 600078, India

<sup>d</sup> Department of Internal Medicine, Taiwan Landseed Hospital, 77 Kuangtai Road, Pingjen City, Tao-Yuan County 32405, Taiwan

<sup>e</sup> Department of Reproduction, National Center for Child Health and Development, 2-10-1 Okura, Setagaya-ku, Tokyo, 157-8535, Japan

<sup>f</sup> Department of Chemical and Materials Engineering, National Central University, No. 300, Zhongda Rd., Jhongli, Taoyuan, 32001, Taiwan. E-mail: higuchi@ncu.edu.tw; Fax: +886-3-2804271; Tel: +886-4227151-34257

<sup>g</sup> R & D Center for Membrane Technology, Chung Yuan Christian University, 200 Chung-Bei Rd., Jhongli, Taoyuan 320, Taiwan

† Electronic supplementary information (ESI) available. See DOI: <https://doi.org/10.1039/d2tb02601e>

‡ These authors contributed equally to this work.

## 1. Introduction

The following cells have been shown to need communication and interaction with extracellular matrix (ECM) proteins, which not only serve as structural components but also guide and support cell fate, adhesion, proliferation, survival and differentiation:<sup>1</sup> (a) human pluripotent stem cells (hPSCs) such as human embryonic stem cells (hESCs) and induced pluripotent stem cells (hiPSCs),<sup>2–6</sup> (b) adult stem cells such as neural progenitor stem cells (NPSCs),<sup>7–9</sup> bone marrow stem cells (BMSCs),<sup>10–16</sup> adipose-derived stem cells (ADSCs),<sup>17–20</sup> Wharton's Jelly-derived stem cells,<sup>21–24</sup> amniotic fluid stem cells<sup>25–28</sup> and dental pulp stem cells,<sup>29–32</sup> and (c) primary cells or differentiated stem cells such as epithelial cells,<sup>33–35</sup> endothelial cells,<sup>36,37</sup> neurons,<sup>38–40</sup> oligodendrocytes,<sup>41–44</sup> retinal pigment cells,<sup>45–47</sup>  $\beta$  cells<sup>48–52</sup> and hepatocytes.<sup>53–57</sup> The binding of the cells with ECM proteins *via* cell adhesion receptors such as integrins activates several signaling pathways that determine cell fate, morphological changes, proliferation and differentiation.<sup>1,58,59</sup>

Typically, xenogenic or allogenic ECM molecules are immobilized on tissue culture polystyrene (TCP) flasks and several

types of scaffolds, hydrogels, implants or nanofibers for adhesion, proliferation, and differentiation of adult stem cells and pluripotent stem cells as well as cells from other tissues. For example, hPSCs can be cultured on Matrigel or Geltrex matrices and recombinant vitronectin or laminin-coated surfaces. Matrigel is derived from mouse Engelbreth–Holm–Swarm sarcomas, and the main components of Matrigel are laminin-111 (laminin-1), laminin-511 (laminin-10) and laminin-332 (laminin-5), collagen and heparan sulfate proteoglycans.<sup>60,61</sup>

Among ECM proteins, laminin and recombinant laminin molecules are very unique ECM proteins compared to other ECM proteins, which are typically used for coating or grafting on TCP dishes, scaffolds, hydrogels, implants and nanofibers to culture hPSCs, NPSCs, hPSC-derived neural cells (including neurons)<sup>62,63</sup> and hPSC-derived cardiomyocytes;<sup>64–68</sup> on collagen- or fibronectin-coated dishes, where hPSCs easily differentiate and/or poorly proliferate.<sup>69,70</sup>

Laminins are high molecular weight proteins (approximately 400–900 kDa) with heterotrimeric chains composed of  $\alpha$ -,  $\beta$ - and  $\gamma$ -chains (Fig. 1), which have five, four, and three genetic variants, respectively.<sup>71–73</sup> The laminin molecules are named according to their heterotrimeric chain composition. Laminin-111 (laminin-1) is composed of  $\alpha 1$ ,  $\beta 1$ , and  $\gamma 1$  chains; laminin-511 (laminin-10) consists of  $\alpha 5$ ,  $\beta 1$ , and  $\gamma 1$  chains;<sup>74,75</sup> laminin-332 (laminin-5) is composed of  $\alpha 3$ ,  $\beta 3$ , and  $\gamma 2$  chains;<sup>76,77</sup> and laminin-521 (laminin-11) contains  $\alpha 5$ ,  $\beta 2$ , and  $\gamma 1$  chains.<sup>78–80</sup>

Although xenogenic or allogenic ECM proteins such as native or recombinant laminin molecules are valuable for the culture of hPSCs, hPSC-derived cells and primary cells, ECM proteins should be produced from human cell lines or *E. coli*, which makes it difficult to chemically define the molecules mixed with ECM proteins after production. The current ECM protein production method cannot avoid the contamination risk of immunogens and pathogens.<sup>1</sup> Furthermore, there exists lot-to-lot variation in ECM proteins. The development of synthetic ECM protein-derived peptides that mimic the biological

and biochemical functions of natural ECMs should be beneficial for academic and clinical application.<sup>1,81–86</sup> Peptides derived from or inspired by specific ECM proteins can work as agonists of each ECM protein receptor. Considering that most ECM proteins influence cell adhesion *via* integrin receptors, many peptides have been developed that bind to specific integrin receptors. In this study, we discuss several peptides, including laminin-derived peptides, for their peptide sequence, immobilization design and reaction method as well as their functions. Various peptide sequences derived from mainly ECM protein molecules, which are used for coating or grafting on dishes, scaffolds, hydrogels, implants or nanofibers for adhesion, proliferation or differentiation of stem cells and their differentiated cells, are summarized in Tables S1,<sup>1,72,87–114</sup> S2<sup>86,88,94,98,105</sup> S3<sup>83,97,98,108,115–124</sup> and S4 (ESI<sup>†</sup>).<sup>86,100,101,110,125–136</sup> The peptides derived from growth factors are also summarized in Table S5 (ESI<sup>†</sup>).<sup>105,137–144</sup>

## 2. Integrin receptors and ECM protein-derived peptides, which promote adhesion, proliferation and differentiation of stem cells

Several designs of peptides derived from ECM proteins have been proposed. In most cases, these bioactive peptides are conjugated to (a) Au surfaces, (b) synthetic or natural films, scaffolds, hydrogels, nanofibers or implants, or (c) proteins with or without alkyl chains or joint segments by physical force (adsorption) or chemical reaction. Here, we first discuss integrin receptors, which bind to bioactive peptides, and then discuss several designs of bioactive peptides.

### 2.1. Integrin structure and function of laminin

In this section, we mainly focus on laminin-derived peptides and integrins for laminin. This is because laminin-immobilized surface can support adhesion of hPSC-derived cardiomyocytes, neural cells, retinal pigment epithelium and some other lineages of the cells. Several bioactive sites of laminin are used for cell adhesion, proliferation and differentiation of hPSCs and NPSCs, such as YIGSR, IKVAV, PDGSR, and RGD.<sup>145,146</sup> However, short peptides, such as RGD, can bind to not only specific integrins for laminin but also other integrins, such as integrins for fibronectin, vitronectin and collagen. Integrins are transmembrane receptors that facilitate the adhesion of cell-ECM proteins.<sup>147</sup> Integrins are heterodimeric molecules that are composed of an  $\alpha$  chain and a  $\beta$  chain that are noncovalently bonded. The  $\alpha$  and  $\beta$  chains are both class I transmembrane proteins that penetrate the plasma membrane and hold cytoplasmic domains. A schematic illustration of typical integrin binding is depicted in Fig. 2, which is based on the literature.<sup>148,149</sup> There are several variances of  $\alpha$  chains and  $\beta$  chains. Currently, at least 24 integrins are known, and human cells express 16 different integrins by a combination of different  $\alpha$  chains and  $\beta$  chains.<sup>150</sup> Integrins, such as  $\alpha 2\beta 1$ ,  $\alpha 5\beta 1$ ,  $\alpha 6\beta 1$ ,

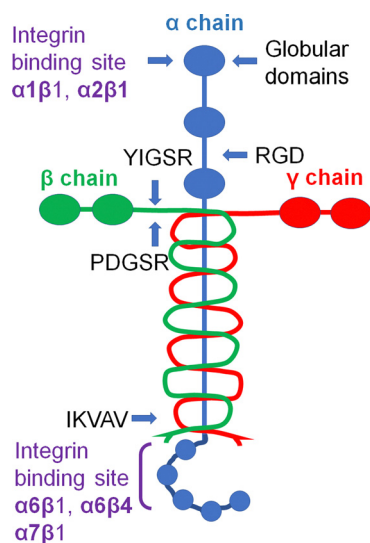


Fig. 1 Schematic structure of the laminin molecule (heterotrimer).

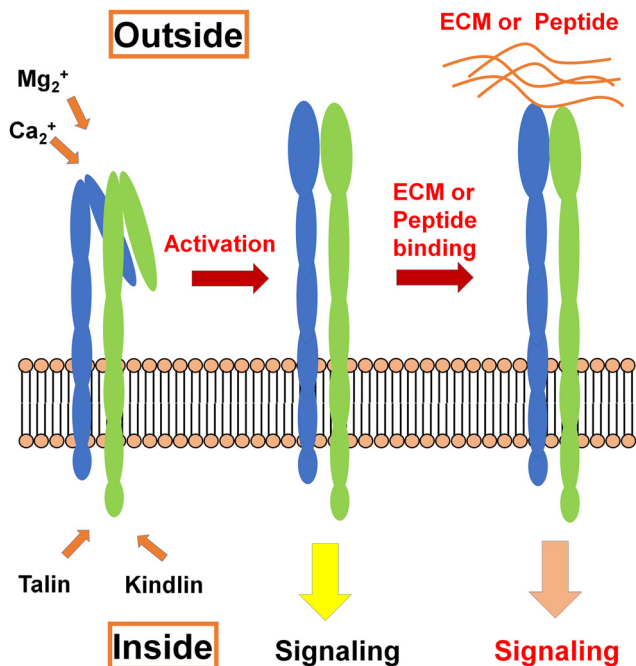


Fig. 2 Schematic illustration of the integrin activation mechanism. Integrins exist in two activation states on the cell surface: a bent inactive state and a straight active state. Integrins are activated from an inactive state by the binding of divalent cations such as  $\text{Ca}^{2+}$  and  $\text{Mn}^{2+}$  at the ectodomain of the integrin, and kindlins and talins bind to the cytoplasmic tail of  $\beta 1$  integrins. Activated integrins bind ECM proteins or ECM-derived peptides, which leads to intracellular signaling and cytoskeletal changes.

and  $\alpha v\beta 5$ , bind to specific ECM proteins. For example, integrin  $\alpha 6\beta 1$  mainly binds to laminin, whereas  $\alpha v\beta 5$  binds to vitronectin. ECM proteins bind to specific integrin receptors, which are summarized in Table S6 (ESI<sup>†</sup>).<sup>87,151</sup>

Fig. 3 shows analytical results of integrin expression and ECM protein expression in hPSCs (H9, HES3, and RiPSCs), hPSC-derived neural progenitor cells (hPSC-derived hNPCs), hPSC-derived endoderm cells (hPSC-ENS), hPSC-derived mesoderm cells (hPSC-MES), and hPSC-derived ectoderm cells (hPSC-ECs), which were investigated by Varun *et al.*<sup>98</sup> hPSCs express most of the integrin  $\alpha$  chain except integrin  $\alpha 8$  and express the integrin  $\beta$  chain. Once hPSCs differentiated into the cell-derived endoderm, mesoderm and ectoderm, the differentiated cells expressed fewer integrins than the hPSCs did, except integrin  $\alpha 8$  (Fig. 3). Integrin  $\alpha 8$  is not expressed in hPSCs, hPSC-derived endoderm cells or hPSC-derived mesoderm cells but is strongly expressed in hPSC-derived ectoderm cells and moderately expressed in hPSC-derived hNPCs. The integrin  $\alpha 8$  expression in hPSC-derived hNPCs, which are ectoderm cells, is not completely the same as that in hPSC-derived ectoderm cells, although there are some similarities in integrin expression between both cell types.<sup>98</sup> The expression difference of integrins in the cells before and after the differentiation of hPSCs can be used for purification of hPSC-differentiated cells from hPSCs on biomaterials immobilized with specific ECM proteins or ECM protein-derived peptides, a method which can serve as cell sorting dishes<sup>66</sup> or for cell affinity chromatography.<sup>152</sup> In Fig. 3,

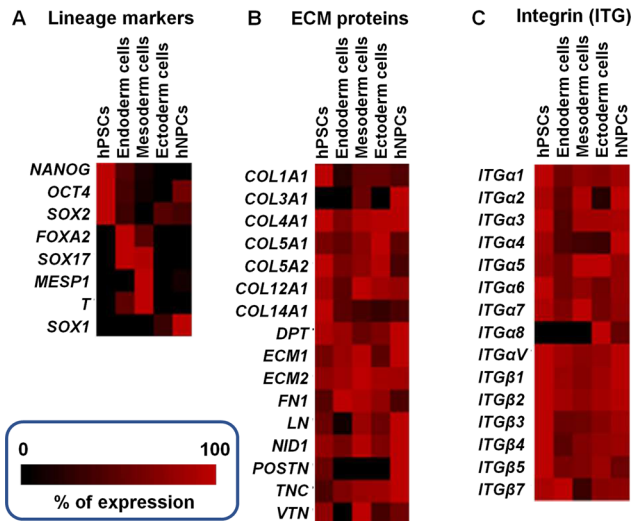


Fig. 3 The expression of lineage markers (A), ECM proteins (B) and integrins (ITG) (C) in hPSCs and hPSC-derived endoderm (EN), mesoderm (ME) and ectoderm (EC) cells analyzed by a quantitative PCR assay. Each data point is illustrated in a heatmap, where black indicates the minimum expression of each gene and red corresponds to the maximum level of each gene. The gene expression levels were normalized to the sample with the highest expression level. Modified from ref. 98, Copyright 2016, Elsevier Ltd.

the expression of several ECM genes in hPSCs and hPSC-derived cells, including hNPCs, is shown. Laminin (LN in Fig. 3) expression is higher than vitronectin (VTN) or fibronectin (FN1) expression on hNPCs, which corresponds to hNPCs preferably attached and cultured on laminin-coated dishes compared to vitronectin-coated dishes or fibronectin-coated dishes.<sup>153,154</sup> The expression levels of ECM proteins and integrin helps to determine which ECM peptides should be immobilized on dishes, nanofibers, hydrogels, implants or scaffolds to be used for specific stem cells and differentiation protocols.

It is necessary to design peptides that target specific integrins for adhesion, proliferation and differentiation of hPSCs and hNPCs. Typically, most researchers graft simple and short RGD peptides onto their polymeric materials to enhance cell adhesion.<sup>145,155–158</sup> Various integrin receptors can bind to RGD, such as  $\alpha 3\beta 1$ ,  $\alpha 5\beta 1$ ,  $\alpha v\beta 1$ ,  $\alpha M\beta 2$ ,  $\alpha IIIb\beta 3$ ,  $\alpha v\beta 3$ , and  $\alpha v\beta 5$ . Specific cells, such as hPSCs or hNSCs, cannot attach to polymeric materials, which are generally grafted with simple RGD peptides. For example, a long sequence containing the RGD peptide KGGPQVTRGDVFTMP is necessary to bind to hPSCs *via*  $\alpha v\beta 5$ ,<sup>68,94,98,159–164</sup> which mimics vitronectin for hPSC adhesion and proliferation. Another RGD peptide, PMQKMRGDVFSF, binds to hPSCs *via*  $\alpha 6\beta 1$ ,<sup>68,88</sup> which mimics the laminin  $\beta 4$  chain for hPSC adhesion and proliferation. Furthermore, the cell adhesion of specific cells depends on the peptide designs, including whether or not RGD is present. Therefore, specific cell binding with high adhesion potential depends on the presence or absence of RGD sequences.

## 2.2. Development and screening of novel bioactive peptides

### 2.2.1. Evolutionarily conserved peptides from ECM proteins.

Several investigators have studied the screening of novel bioactive

sequences of cell adhesion peptides using high throughput or conventional methods. Jia *et al.* identified laminin-derived peptides expressing extensive support for endothelial cell adhesion and vascular formation by leveraging motif analysis of an evolutionarily conserved peptide sequence containing RGD in the laminin ( $\alpha 1$ ) chain.<sup>87</sup> They studied peptide sequences of RGD-containing domains of laminin subunits from *Euarchontoglires* species (Fig. 4A). They analyzed the probability of evolutionary conservation of the sequence and displayed each amino acid position in the peptide sequences utilizing a bitmap-based motif assay (Fig. 4B). They identified the highly conserved sites around the RGD region and then determined the specific amino acids, which showed the highest frequency in each position. From this method, six highly conserved RGD-containing sequences from laminin were selected, which are shown in Table S7 (ESI†).<sup>87</sup> Two different novel peptides containing RGD and RGD mimicking peptide (RAD) were selected: GTFALRGDNP (RGD version,  $\alpha 1$ -1) and GTFALRADNP (RAD version).

They evaluated these peptides obtained from the analysis of evolutionary conservation of peptide sequences around the RGD motif for human endothelial cell (human umbilical vein endothelial cell, HUVEC) adhesion on the microarrays of hydrogels prepared with methacrylated peptides and GGGG (G; glycine) as a joint segment. The methacrylated peptides are mixed with polyethylene glycol (PEG) diacrylate and the mixed solution was spotted and polymerized under UV light to generate microarrays spotted with the hydrogels grafted with these peptides.<sup>87</sup> The hydrogels containing the  $\alpha 1$ -1 peptide showed better HUVEC attachment than the hydrogels containing other sequences of the peptides. The hydrogels containing  $\alpha 1$ -1 peptide promoted better vascular network formation of HUVECs compared to the hydrogels containing  $\beta 4$  peptide (RGDVFSPGMVHG) as well as the hydrogels containing A99 (QAGTFALRGDNOQG) and PA26 (FALRGDNP) peptides, which are laminin-derived peptides reported previously. The therapeutic effect of the injectable alginate hydrogels containing

$\alpha 1$ -1 peptides with and without MMPQK (a site that is degradable by matrix metalloproteinase (MMP) enzymes) on vascular network formation was evaluated using hindlimb ischemia mice, where the MMPQK peptide promotes ECM cleavage and facilitates remodeling of ECM networks, which is important for tissue regeneration.<sup>87</sup> Extensive enhancement in blood restoration in the hindlimb ischemia mice (60% recovery by day 28) was observed by injection of the hydrogels containing  $\alpha 1$ -1 and MMPQK peptides compared to the injection of the hydrogels containing  $\alpha 1$ -1 peptides only or the hydrogels containing RGDS and MMPQK peptides; interestingly, the hydrogels containing RGDS and MMPQK peptides have been widely reported to promote vascular network formation.<sup>165–167</sup> Significant enhancement of artery and capillary blood vessel formation and a decrease in muscle degeneration and fibrotic area were observed in hindlimb ischemia mice injected with hydrogels containing  $\alpha 1$ -1 and MMPQK peptides.<sup>87</sup>

The superior characteristics of endothelial cell adhesion and vascular formation potential of the  $\alpha 1$ -1 peptide may be explained as  $\alpha 1$ -1 peptides allow integrin receptors to not only target laminin but also fibronectin. It has also been found that some long sequences of peptides containing RGD are necessary to generate specific and unique functions of specific cell adhesion and tissue regeneration. For example, the  $\alpha 1$ -1 (GTFALRGDNP) peptide contains 10 amino acids, whereas the simple RGD peptide contains only 3 amino acids. Peptides with long sequences likely fix specific stereo structures (3D conformations), whereas single peptide chains, such as RGD, have flexible structures and cannot fit into specific integrin receptors with high affinity. Some interesting future work would be to evaluate an evolutionarily conserved peptide sequence containing RGD (and other small integrin binding peptides) using not only laminin chains such as laminin  $\alpha 3$ ,  $\alpha 4$ ,  $\alpha 5$ ,  $\beta 1$ ,  $\beta 4$ ,  $\gamma 1$ ,  $\gamma 2$  and  $\gamma 3$  chains but also other ECM proteins such as fibronectin and vitronectin.

**2.2.2. Modified ECM protein-derived peptides.** Park *et al.* designed several new peptides originating from vitronectin using *in silico* docking simulation. In this simulation, a vitronectin-derived peptide (KGGPQVTRGDVFTMP) and the crystal structure of integrin were used as the original ligand and target receptor, respectively.<sup>168</sup> Then, a genetic algorithm was performed to develop strongly binding vitronectin-derived peptides. Some peptides from the vitronectin sequence supported attachment and long-term culture of hPSCs from experimental results. Consequently, one peptide was identified with a binding affinity of  $-8.0 \text{ kcal mol}^{-1}$  (VNP1; KGGPQVTRGDYCTFP) and another with a binding affinity of  $-7.8 \text{ kcal mol}^{-1}$  (VNP2; KGGPGVTRGDFTFP).<sup>168</sup> VNP2, in particular, promoted the differentiation of hPSC-derived oligodendrocyte precursor cells into oligodendrocytes more effectively than other peptides when immobilized on the dishes. This simulation method can lead to the proposal of a variety of different peptides from existing ECM protein-derived peptides, which are better for binding to specific integrin receptors. In the future, it would be useful to research whether this method can be applied to other existing ECM protein-derived peptides.

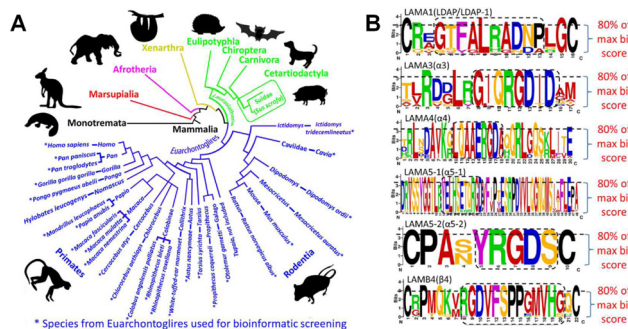


Fig. 4 Evolutionarily conserved motif analysis of laminin-derived RGD peptides from species in the Euarchontoglires group. (A) Schematic illustration of the species in *Euarchontoglires* for conserved motif analysis of laminin-derived RGD peptides. (B) Motif analysis of the highly conserved sequences among Euarchontoglires species. Dashed-line boxes from the plots indicate the highly conserved positions around RGD. The repetitions of each amino acid is indicated by the size of the letter. Reproduced from ref. 87 under a Creative Commons Attribution NonCommercial License 4.0.



**2.2.3. Novel peptides from the selection of phage-derived peptides.** One strategy to find novel short peptides that work as agonists of integrin receptors on cells is to find evolutionally conserved peptide sequences around RGD, which was investigated by Jia *et al.*,<sup>87</sup> as discussed previously. Another strategy to find novel peptides is library-based selection of peptides expressed on bacteria that bind to specific cell-binding receptors. This method is similar to the method used to generate DNA aptamers targeting specific antigens, which are purified using the systematic evolution of ligands by exponential enrichment (SELEX) method.<sup>169–172</sup> Ramasubramanian *et al.* found short peptides working as agonists for the  $\alpha 6$  integrin receptor, which is a laminin receptor of hPSCs, from bacterial peptide display libraries.<sup>60</sup>

In this method, the bacteria were genetically modified to express green fluorescence protein (GFP) and CPX protein fused with short peptide sequences, where the short peptide sequences were a variety of linear 15-mer sequences (X15, where X is any amino acid) or a variety of cyclized 7-mer sequences of the form of X2CX7CX2 (where X is any amino acid), depending on the bacteria,<sup>60</sup> where cysteine (C) molecules in the sequence bind to each other to generate a cyclic peptide. The process of untargeted selection, which does not target the  $\alpha 6$  integrin receptor but targets any receptors on hESCs (H1), proceeds in four cycles. After binding of the bacteria to hESCs, the bacteria-bound hESCs were isolated, and the selected bacteria that can bind to hESCs were cultured and expanded (Fig. 5A).<sup>60</sup> These processes were repeated four times. In the subsequent targeted peptide selections for  $\alpha 6$  integrin receptor, hESCs were first treated with the blocking antibody for  $\alpha 6$  integrin subunit (Fig. 5B).<sup>60</sup> Then, the antibody-blocked hESCs were coincubated with the bacterial library, which was selected in the previous untargeted selections. The unbound bacteria in the supernatant were collected (negative selection) and incubated (Fig. 5B). Finally, the peptides expressing the unbound bacteria were analyzed.<sup>60</sup> Three cyclic peptides, 7C-1, 7C-2 and 7C-12, and one linear sequence, 15-23, which have highly selective binding to the  $\alpha 6$  integrin of hESCs, were selected for further analysis; peptides 7C-1 and 7C-2 contained an RGD-like moiety, DGR. The identified peptides, which are summarized in Table S8 (ESI<sup>†</sup>), could bind to the  $\alpha 6$  integrin receptor of hPSCs with a sub- $\mu\text{M}$  dissociation constant, which is the same order of magnitude as the dissociation constant of laminin.<sup>60</sup>

hESCs adhered to the surface immobilized with cyclic peptides 7C-1, 7C-2 and 7C-12 with an 80–90% adhesion rate and showed stronger hESC adhesion on the surface immobilized with the linear peptide, 15–23.<sup>60</sup> This is because cyclic peptides lose their conformational entropy, which leads to enhanced fitting between the peptide and the integrin receptor. In particular, hESCs on the surface immobilized with 7C-1 showed higher adhesion than those on the surface immobilized with other cyclic peptides (7C-2 and 7C-12) or the linear peptide (15–23) and expressed the pluripotent protein of Oct3/4 on levels comparable to cells on dishes coated with Matrigel (a gold standard material for hPSC culture). It should be noted that hESCs can adhere to peptide-immobilized surfaces with even a very dilute peptide density (28 pmol  $\text{cm}^{-2}$ ). However, the density of immobilized bioactive peptides on

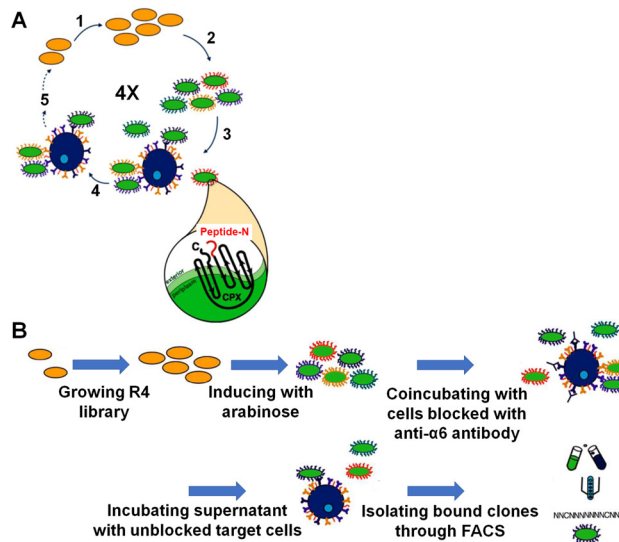


**Fig. 5** Untargeted and targeted screening for hPSC-binding peptides. (A) Untargeted screening for hPSC binding peptides. The bacterial display scheme is utilized to determine novel hPSC-binding peptides. The bacterial libraries are (1) cultured and (2) induced to express *algGFP* and a unique peptide variant on the bacterial surface. Each peptide, fused to the N-terminus of the circularly permuted outer membrane protein (inset), can interact with specific integrin receptors on the hPSC surface. Panning is performed by (3) incubating peptide-expressing bacteria with hPSCs, (4) allowing for binding events to occur and (5) eliminating unbound clones. (B) Targeted screening for integrin-binding peptides. The bacterial display scheme utilized to identify peptides that bind hPSCs *via* specific integrins. Bacterial libraries are sequentially panned against two target hPSCs: (1) hPSCs with the target receptor blocked by antibodies, which ablate receptor binding (negative selection), and (2) unblocked hPSCs (positive selection). Bacterial clones, which cannot bind the target during negative selection but bind during positive selection, are considered to have specific integrin specificity. Copyright 2021. Adapted from ref. 60 with permission from the American Chemical Society.

synthetic material surfaces should be greater than or equal to 600 pmol  $\text{cm}^{-2}$  for hESC cultures to attain a proliferation speed similar to that of hESCs cultured on Matrigel-coated dishes.

The cyclic peptide 7C-1, which was found to be the best peptide for hPSC culture in the study, was conjugated with alkanethiol, and self-assembled monolayers (SAMs) were prepared on gold-coated plates.<sup>60</sup> SAM surfaces were prepared using not only 7C-1 peptides but also alkanethiol-conjugated bspRGD(15), which has integrin- and glycosaminoglycan-binding motifs (a 15-amino-acid ligand for  $\alpha V\beta 3$ -integrin), and alkanethiol-conjugated Ag73, which is a syndecan-1 and  $\beta 1$ -integrin binding peptide. The hiPSCs cultured on the SAM surface prepared with a mix of three peptides (20% cyclic 7C-1, 40% bspRGD(15), and 40% Ag73 peptides) showed much better characteristics than any SAM surface coated with only one or two peptides.<sup>60</sup> This is because the SAM surface coated with three peptides activates not only  $\alpha 6$ -integrin but also other surface receptors to facilitate hiPSC adhesion. However, the maximum culture period of the study was a single 5 days passage. It is necessary to evaluate more long-term culture (*e.g.*, > 10 passages) of several hiPSC and hESC lines on a triple-peptide-grafted surface to evaluate the capacities of the three peptides as binding sites of

hPSC in their proliferation. However, the idea to use multiple ECM protein-derived peptides, which target multiple integrin receptors, might be useful for future hPSC culture and differentiation into specific lineages of cells on biomaterials immobilized with multiple ECM protein-derived peptides.

The peptides should be immobilized on 2D or 3D materials for adhesion, culture, proliferation, and differentiation of primary cells, stem cells and progenitor cells. To do so, the peptides are covalently immobilized (peptide-conjugation method) or are adsorbed (peptide-coating method) on cell culture materials. In most cases, peptides are covalently conjugated on cell culture materials such as TCP plates, polymeric films, gold-coated materials, nanofibers, implants, scaffolds and hydrogels. The coating method of the peptides and the chemical reaction of the immobilization of peptides on 2D and 3D materials are discussed in the following section.

### 3. Immobilization method of ECM protein-derived peptides

#### 3.1. Methods of coating cell culture materials with peptides

Peptides with or without modification can be coated on TCP plates, polymeric films, implants or scaffolds using the coating method. Although ECM proteins such as recombinant vitronectin, laminin-511, or laminin-521 are frequently immobilized on TCP dishes for hPSC culture and differentiation by the coating method, some researchers have also immobilized non-modified peptides.<sup>72,92,98,108,129,173–179</sup> There are also some reports that peptides were conjugated with synthetic polymers or proteins by chemical or genetic engineering methods; the resulting polymers are used as coating materials. Several studies in which stem cells are cultured on peptide-coated surfaces are summarized in Table S9 (ESI<sup>†</sup>).<sup>89,92,98,108,129,150,173,174,177–187</sup> These investigations are discussed in more detail as follows.

**3.1.1. Native linear peptides as coating materials.** Short peptides (sequences of fewer than 6 amino acids), such as RGD, IKVAV, YIGSR, RGD, RGDS, and RGDSP, are generally difficult to adhere to conventional 2D and 3D materials in because of the high entropy of the peptides in solution compared to the peptides adsorbed on the material surface. The high entropy of the short peptides originates from the high movement of the peptides in the solution phase. Therefore, most researchers designed relatively longer sequences of peptides, including hydrophobic and aromatic rings and/or charged amino acids, for hydrophobic and/or electrostatic binding to the material surface.

Puah *et al.* designed peptides by combining the bioactive peptide site from ECM proteins, including laminin-derived peptides YIGSR and IKVAV (Table S1, ESI<sup>†</sup>).<sup>92</sup> The combined peptides (YIGSRWYQNMIRIKVAV, QHREDGSYIGSRIKAVV, WQPPRARIYIGSRIKAVV, DGEARGDSPKRSR) (Fig. 6) were coated on multilayer graphene oxide (mGO) with a relatively low coating concentration of the combined peptide solution (50  $\mu\text{M}$ , or 105  $\mu\text{g mL}^{-1}$  for YIGSRWYQNMIRIKVAV).<sup>92</sup> This is because the combined peptides contain 3–4 positively charged amino acids and 0–3 aromatic amino acids on each combined



Fig. 6 The combined peptide sequences with and without a joint segment (GGGG), which are derived from laminin.

peptide, which contribute to peptide attachment to the mGO surface by electrostatic forces and  $\pi$ - $\pi$  interactions. Wharton's Jelly-derived mesenchymal stem cells (WJ-MSCs) showed better proliferation and facilitated osteogenic differentiation on peptide-coated mGO surfaces compared to native mGO surfaces.<sup>92</sup> The combined peptide was effective in facilitating a high proliferation and desired differentiation direction of WJ-MSCs. However, it would have been more valuable to compare the combined peptides to the mixture of peptides (from which the combined peptides are derived) from a single active site and with similar molecular weight (Fig. 6). With such a comparison, the effect of the multiple bioactive sites of the combined peptides on WJ-MSC proliferation and differentiation could be clarified. Furthermore, a joint segment (GG, GGG or GGGG) might be necessary between each bioactive site in the peptides (Fig. 6). For example, the peptides DGEAGGRGDSPPGGKRSR or DGEAGGGGRGDSPPGGGKRSR might be more effective in guiding the proliferation and differentiation of WJ-MSCs than the original peptide DGEARGDSPKRSR.

Varun *et al.* investigated the expression of ECM proteins and integrin in hPSCs, hPSC-derived endoderm, mesoderm and ectoderm cells, and hNPCs, as described previously (Fig. 3).<sup>98</sup> From these data, they designed 18 peptides derived from bioactive sites of laminin  $\alpha$ 1 (5 peptides), laminin  $\beta$ 1 (1 peptide), laminin  $\gamma$ 1 (4 peptides), vitronectin (2 peptides), fibronectin (4 peptides), and collagen (1 peptide), as described in Tables S1, S2 and S7 (ESI<sup>†</sup>). Only four peptide-coated dishes supported hNPC adhesion and proliferation for 3 days of culture; the hNPCs coated on the peptide-coated dishes showed similar characteristics (cell morphology and cell numbers) to hNPCs on laminin-coated dishes. The four favorable peptides are (a) CGGTWYKIAFQRNRK (laminin  $\alpha$ 1-derived peptide), which binds to integrin  $\alpha$ 6 $\beta$ 1 and  $\alpha$ 2 $\beta$ 1; (b) CDIRVTLNRL (laminin  $\gamma$ 1-derived peptide), which binds to integrin  $\alpha$ 6 $\beta$ 1; (c) CKGGPQVTRGDVFTMP (vitronectin-derived peptide), which binds to integrin  $\alpha$ v $\beta$ 5 and  $\alpha$ 5 $\beta$ 1; and (d) CGKKQRFHRNRK (vitronectin-derived peptide, HBP-1C), which binds to integrin  $\alpha$ v $\beta$ 5.<sup>98</sup>

The four selected peptides were further investigated to determine whether hNPCs can be cultured on the peptide-coated dishes for a long time (up to 10 passages). hNPCs can expand on vitronectin-derived peptide (CGKKQRFHRNRK)-coated dishes (HBP-1C-coated dishes) with less differentiation and similar morphologies to hNPCs cultured on laminin-coated dishes. Furthermore, hNPCs can differentiate into neuronal cells in HBP-1C-coated dishes in neuronal differentiation medium.

Several neuronal markers, such as  $\beta$ 3-tubulin, microtubule-associated protein 2 (MAP2), neurofilament-68 (NF-L), and  $\gamma$ -aminobutyric acid (GABA), were expressed similarly in the cells derived from hNPCs cultured on HBP-1C-coated dishes and on laminin-coated dishes. Therefore, the authors concluded that the vitronectin-derived peptide CGKKQFRHRNRKG is effective as a coating material for hNPC culture and proliferation and differentiation into neurons.

However, it should be noted that the minimum concentration of the peptide (CGKKQFRHRNRKG) coating solution that they used was 100  $\mu$ M, corresponding to 177.1  $\mu$ g mL<sup>-1</sup>, whereas the concentration of laminin coating solution was 5  $\mu$ g mL<sup>-1</sup>. This result indicates that the concentration of the peptide solution should be 35 times higher than that of the ECM protein solution to receive these results.

Hennesy *et al.* prepared collagen I mimetic peptide (DGEA, P15 (GTPGPQIAGQAGVV), and GFOGER)-coated hydroxyapatite disks using 1000  $\mu$ g mL<sup>-1</sup> peptide solution to investigate human bone marrow stem cell (hBMSC) attachment and differentiation into osteoblasts.<sup>173</sup> hBMSCs adhered better and showed more efficient differentiation into osteoblasts on hydroxyapatite disks coated with DGEA and P15 compared to uncoated hydroxyapatite disks or disks coated with GFOGER.<sup>173</sup>

It is known that stem cells cultured on tissue-specific ECM can differentiate into specific tissue cells with high efficiency.<sup>187–196</sup> Therefore, Dorgau *et al.* prepared decellularized ECM peptides from the neural retina and retinal pigment epithelium (RPE) of adult bovine eyes by using surfactant treatment.<sup>187</sup> They generated rod photoreceptors with high efficiency from hPSCs using decellularized ECM peptides in the differentiated medium. Furthermore, the addition of decellularized ECM peptides to the differentiation medium led to the enhancement of ribbon synapses and light-responsive retinal organoids. Although decellularized ECM peptides derived from specific tissues are promising bioactive agents for controlling cell differentiation, decellularized ECM peptides are not chemically defined, and it is expected that many different types of peptides (with and without modification of several types of glycosaminoglycans) exist in the decellularized ECM peptides. Identifying the peptides that most effectively guide hPSCs into rod photoreceptors and light-responsive retinal organoids would be valuable in regenerative therapy of eye disease.

**3.1.2. Linear modified peptides with two different functional sites as coating materials.** Sharmin *et al.* prepared genetically engineered peptides derived from laminin, p20 (RNIAEIIKDI) and RGD, which were designed to be combined with elastin-like polypeptide (ELP, (APGVGV)<sub>12</sub>) (see Tables S1, S9, ESI† and Fig. 7).<sup>108</sup> The p20 and RGD peptides contribute to cell attachment, whereas ELP promotes anchorage of the engineered peptide to the cell culture dishes or scaffolds. Saturated engineered peptide adsorption was observed on polystyrene (PS) dishes with coating concentrations of 500 nM (6.4  $\mu$ g mL<sup>-1</sup>, 2.4  $\mu$ g cm<sup>-2</sup>) for the ELP-RGD-ELP-p20 (ERE-p20) peptide and 750 nM (5.0  $\mu$ g mL<sup>-1</sup>, 2.3  $\mu$ g cm<sup>-2</sup>) for the ELP-p20 (E-p20) peptide (Fig. 7).<sup>108</sup> The coating concentrations of these ELP peptides were similar to of the concentrations of ECM

p20, RNIAEIIKDI (Peptide derived from Laminin)  
E, (APGCGC)<sub>12</sub> (Elastin like peptide)

E-p20, (APGCGC)<sub>12</sub>-RNIAEIIKDI  
ERE, (APGCGC)<sub>12</sub>-RGDSP-(APGCGC)<sub>12</sub>  
ERE-p20, (APGCGC)<sub>12</sub>-RGDSP-(APGCGC)<sub>12</sub>-RNIAEIIKDI

A99, AGTFALRGDNPQG (Peptide derived from Laminin  $\alpha$ 1 chain)  
I30, MG(VPGIG)<sub>30</sub>Y (Elastin like peptide)

A99-ELP-R, MAGTFALRGDNPQGGMG(VPGIG)<sub>30</sub>Y

Fig. 7 The genetically engineered peptides derived from laminin, p20 (RNIAEIIKDI) and RGD with elastin-like peptide.

coatings such as recombinant vitronectin (5.0  $\mu$ g mL<sup>-1</sup>).<sup>197</sup> At a low peptide solution concentration, the peptide containing two domains of the anchorage peptide ELP (ERE-p20) can be more easily adsorbed and saturated on TCP dishes than the peptide containing just one domain of ELP (E-p20) can. Mouse iPSCs (miPSCs) could attach to both engineered peptide-coated surfaces (ERE-p20- and E-p20-coated) with a cell binding efficiency similar to that of laminin-coated dishes.<sup>108</sup> The miPSCs were differentiated into neuronal cells. The cells were successively differentiated into neuronal lineage cells, which were cultured on dishes coated with ERE-p20 and E-p20. The neurites from neurospheres adhered to E-p20- and ERE-p20-coated dishes were thicker and the number of primary neurites and branchpoints were larger than those on laminin-coated dishes.<sup>108</sup> Furthermore, the expression of MAP2 (a neuronal marker) and nestin (a neural stem/progenitor cell marker) in the cells on E-p20-coated and ERE-p20-coated dishes was 2.5-fold and 2.0-fold higher than that on laminin-coated dishes, respectively.<sup>108</sup> The engineered peptide prepared from the molecular design of a combination of the laminin-derived peptide (p20) and the anchorage peptide (ELP) contributes to the efficient adhesion of miPSCs and optimal differentiation of miPSCs into the neuronal lineage of the cells and thus can be used as a coating material.

A similar design of the engineered peptides was developed by several researchers.<sup>175,176</sup> For example, Truong *et al.* developed the engineered peptide (A99-ELP-R), which contains laminin  $\alpha$ 1 chain-derived peptide (A99, AGTFALRGDNPQG) and elastin-like peptide ((VPGIG)<sub>30</sub>) with a GMG joint segment (Fig. 7).<sup>175</sup> Lee *et al.* engineered globular domains 1–3 of laminin  $\alpha$ 5 with fusion to ELP,<sup>176</sup> an engineered peptide that should be called a protein because of its high molecular weight (70 kDa). The TCP dishes coated with 1  $\mu$ g mL<sup>-1</sup> of the engineered peptide (protein) could support hMSC adhesion with favorable stem cell characteristics.

Lee *et al.* designed a peptide combined with two different peptide domains: one peptide is bone morphogenetic protein-2 (BMP-2) domain, KIPKACCVPTLSAISMLYL, and the other peptide is hydroxyapatite-binding domain. The engineered peptide is inspired by N-terminal osteocalcin having an  $\alpha$ -helix structure and sequences of the form  $\gamma$ EPRR $\gamma$ EVA $\gamma$ EL,  $\gamma$ EPRRVAAL, EPRREVAEL and EPRRAVAAL (Table S9, ESI†),<sup>177</sup> where  $\gamma$ E is  $\gamma$ -carboxylated glutamic acid. The original N-terminal osteocalcin domain,  $\gamma$ EPRR $\gamma$ EVC $\gamma$ EL, is modified with (i) alanine (A) instead of cysteine (C) and (ii) glutamic acid



(E) or alanine (A) instead of  $\gamma$ E in some peptides, which may affect whether the  $\alpha$ -helix structure is more or less stable compared to the original N-terminal osteocalcin domain. The sequence of four continuous alanine residues, AAAA, was used as a joint segment between two different peptide domains, which contributes to the  $\alpha$ -helix structure. A hydroxyapatite layer grown on poly(lactide-*co*-glycolide) (PLGA) films was coated with the designed peptides eBGa3 (KIPASSVPTELSASTLYL-AAA- $\gamma$ EPRR $\gamma$ EVC $\gamma$ EL), eBGa1 (KIPASSVPTELSASTLYL-AAA- $\gamma$ EPRAVAAL), eBGu3 (KIPASSVPTELSASTLYL-AAA-EPRREVAEL) and eBGu1 (KIPASSVPTELSASTLYL-AAA-EPRRAVAAL) with a 100  $\mu\text{g mL}^{-1}$  peptide solution.<sup>177</sup> Chemical schemes of base polymeric materials for coating or grafting ECM protein-derived peptides discussed in this review are shown in Fig. 8.

The saturated adsorbed amount of the peptides depended on the modified peptide of N-terminal osteocalcin. The amount of the peptide bound on the hydroxyapatite grown on the PLGA surface was in the following order: eBGa3  $\gg$  eBGa1  $\gg$  eBGu1 = eBGu3  $\gg$  KIPASSVPTELSASTLYL.<sup>177</sup> Similar to the saturated adsorption amount of the peptides, the peptides released from the hydroxyapatite formed on PLGA films in aqueous solution. The peptide eBGa3 was released slowly (only 16% release after 70 days), whereas the peptides eBGu1 and eBGu3 were released much faster (more than 93% was released after 5 days).<sup>177</sup> These results indicate that  $\gamma$ EPRR $\gamma$ EVA $\gamma$ EL in eBGa3 generates the most stable  $\alpha$ -helix structure. The hydroxyapatite (formed on PGLA film) coated with eBGa3 promoted the efficient differentiation of hBMSCs into osteoblasts in the osteogenic medium. Osteogenic differentiation of hBMSCs was highest on hydroxyapatite (formed on PGLA film) coated with eBGa3 than that of hBMSCs coated on TCP dishes or hydroxyapatite (formed on PGLA film) without a coating or with a coating of other peptides.<sup>177</sup>

Studying the combination of different functional peptides with joint segments, such as the combination of anchoring

peptides and bioactive peptides with joint segments, should be useful to develop sophisticated bioactive peptides as coating materials.

Another type of peptide design having a combination of two different functional peptides is EEEEEERGD, which was developed by Sawyer *et al.* (Table S9, ESI $\dagger$ ), where E7 was designed to enhance the anchorage of the peptides by ionic interaction with the hydroxyapatite biomaterial surface.<sup>178</sup> The hydroxyapatite, which was precoated with a low concentration of EEEEEERGD (1–10  $\mu\text{g mL}^{-1}$ ), was subsequently coated with 100% FBS and promoted hBMSC adhesion and spreading compared to the hydroxyapatite sequentially coated with RGD and FBS (without the pretreatment of EEEEEERGD). Compared to culture on EEEEEERGD-coated hydroxyapatite, the introduction of a joint segment such as GGGG in the coating peptide (resulting in EEEEEERGD-GGGG-RGD-coated hydroxyapatite) may improve hBMSC adhesion, spreading and differentiation characteristics.

**3.1.3. Cyclic peptides as coating materials.** Some researchers have used cyclic peptides, which do not combine with proteins, as coating materials to enhance the attachment, spreading and differentiation of stem cells, progenitor cells, and primary tissue cells.<sup>174</sup>

Sawyer *et al.* used two peptide coatings to improve hBMSC attachment and spreading on hydroxyapatite for bone regeneration.<sup>174</sup> The peptide coatings contain unnatural amino acids: one is a linear peptide of GRGDdSP (D-serine (dS) is used), and the other is a cyclic peptide of G(Pen)GRGDSPCA, where (Pen) indicates penicillamine; a thiol group in the penicillamine and a thiol group in serine are conjugated to make a cyclic peptide in the G(Pen)GRGDSPCA peptide (Fig. 9). The coating of GRGDdSP or G(Pen)GRGDSPCA alone on the hydroxyapatite surface is not enough to promote cell attachment and spreading.<sup>174</sup> hBMSCs extensively attached and spread on hydroxyapatite when the surface was precoat with low peptide concentrations, such as 1 or 10  $\mu\text{g mL}^{-1}$ , and subsequently coated with 100% fetal bovine serum (FBS). Interestingly, a high concentration of peptide precoating (100 or 1000  $\mu\text{g mL}^{-1}$ ) inhibited cell attachment on the hydroxyapatite surface prepared with the peptide/FBS coating.<sup>174</sup> This finding can be explained as follows: GRGDdSP binds to the binding site (integrin receptor) of fibronectin, and G(Pen)GRGDSPCA binds to the binding site of

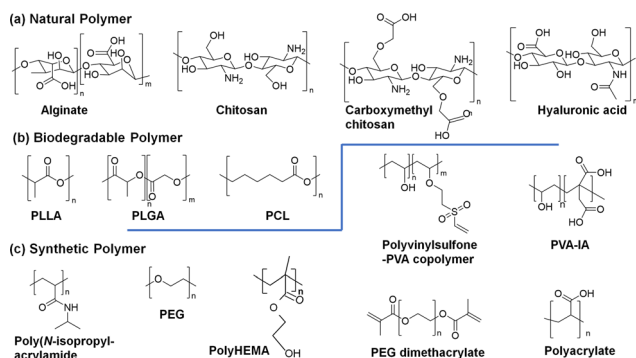


Fig. 8 Chemical schemes of (a) natural polymers (alginate, chitosan, carboxymethyl chitosan and hyaluronic acid), (b) biodegradable polymers (poly-L-lactic acid [PLLA], poly(lactic-*co*-glycolic acid) [PLGA] and poly- $\epsilon$ -caprolactone [PCL]) and (c) synthetic polymers (polyHEMA), poly(*N*-isopropylacrylamide), polyethyleneglycol [PEG], polyethyleneglycol dimethacrylate [PEG dimethacrylate], polyacrylate, polyvinylsulfone-polyvinyl alcohol (PVA) copolymer, poly(vinylalcohol-*co*-itaconic acid) [PVA-IA]), which are used as base polymeric materials for coating or grafting ECM protein-derived peptides.

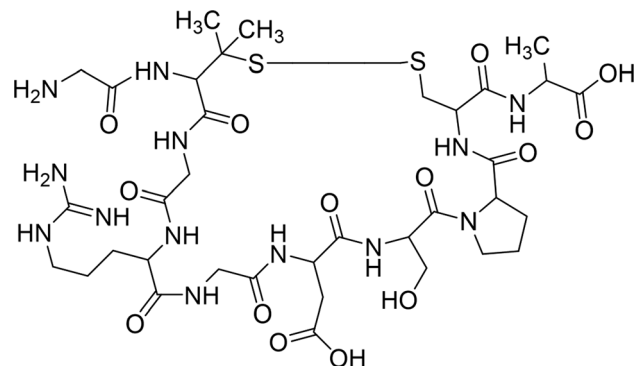
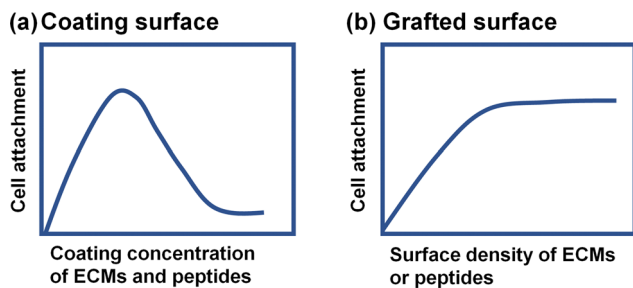


Fig. 9 Chemical structure of a cyclic peptide of G(Pen)GRGDSPCA.





**Fig. 10** Cell attachment tendency on the materials (a) coated or (b) grafted with ECM proteins or ECM protein-derived peptides. (a) Cell attachment shows the maximum point with increasing coating concentration of ECM proteins or ECM protein-derived peptides. (b) Cell attachment shows a plateau with increasing coating concentration of ECM proteins or ECM protein-derived peptides.

vitronectin. Too high of a single peptide density on the surface will inhibit the usage of other binding sites of ECM proteins and glycosaminoglycan or generate free peptides in the culture medium. The free peptides are released from the hydroxyapatite surface, working as inhibitors of the cell binding on the hydroxyapatite surface. This is likely the reason that GRGDdSP was used instead of GRGDSP (all amino acids are *L*-isomers) to reduce the binding of the free peptide on hBMSCs as an inhibitor. He *et al.* also reported that titanium (Ti) implants coated with the LL-37 peptide (LLGDFFRKSKEKIGKEFKRIVQRIKDFLRNLPRTES), a cationic antimicrobial peptide; the medium ( $50 \mu\text{g mL}^{-1}$ ) or low ( $5 \mu\text{g mL}^{-1}$ ) concentration of the peptide promoted rat BMSC expansion and viability, while the high concentration ( $100 \mu\text{g mL}^{-1}$ ) did not.<sup>129</sup> Therefore, the covalent binding of the bioactive peptides on cell culture materials is important to prevent the bioactive peptides from being released and acting as inhibitors (Fig. 10).

There was no significant difference in the usage of GRGDdSP and G(Pen)GRGDSPCA peptides for hBMSC attachment and spreading. If hPSCs were used instead of hBMSCs, hPSC attachment and proliferation might show more distinct differences for different peptide coatings, especially for comparison of single peptide-coated surface and mixed peptide-coated surface, allowing better evaluation of the peptides.

### 3.1.4. Chemically modified peptides as coating materials.

In some previous studies,<sup>68,94,161,183,185,198</sup> several chemically modified peptide sequences from ECM proteins were designed and grafted onto polymers or biomacromolecules as coating materials (Tables S1, S2 and S9, ESI<sup>†</sup>). Stem cells were then cultured on the surfaces coated with the peptide-conjugated.

Vida *et al.* prepared polyamidoamine RGD peptide-conjugated dendrimers (Fig. 11),<sup>183</sup> which were coated on PS dishes for hBMSC culture; (RGDC)<sub>8</sub>-polyamidoamine dendrimer and polyamidoamine dendrimer-(CRGD)<sub>8</sub> were used in the study. hBMSCs on the dishes coated with (RGDC)<sub>8</sub>-polyamidoamine dendrimer adhered better and proliferated more extensively than those cultured on the dishes coated with polyamidoamine dendrimer-(CRGD)<sub>8</sub>.<sup>183</sup> If the joint segment of GG, GGG or GGGG were to be introduced between RGD peptide and polyamidoamine and if RGDSP and not RGD is selected as a bioactive peptide (*e.g.*, (RGDSP-GGGG-C)<sub>8</sub>-polyamidoamine dendrimer), the cell adhesion and

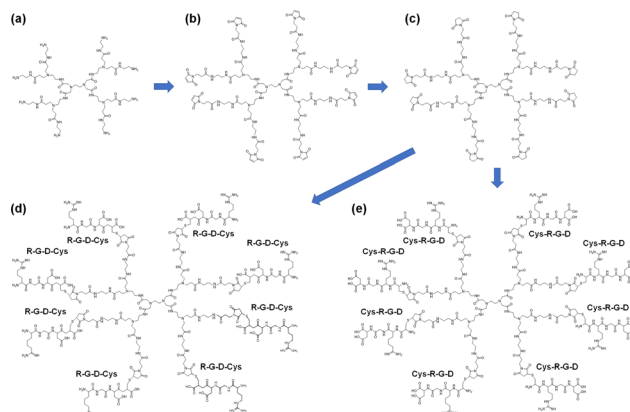


**Fig. 11** Preparation and chemical scheme of polyamidoamine RGD peptide-conjugated dendrimers.

differentiation might be improved from what was observed in the study.

Yang *et al.* designed a clickable mussel-inspired peptide (3,4-dihydroxy-*L*-phenylalanine-polyethylene glycol-azide ((DOPA)<sub>4</sub>-PEG5-azide)) using polydopamine,<sup>198</sup> where clickable mussel-inspired peptides were conjugated on the hydroxy group of a titanium oxide (TiO<sub>2</sub>)-coated stainless stent surface using mussel-inspired adhesion (Fig. 12). Subsequently, NO-generating organoselenium (dibenzylcyclooctyne (DBCO)-SeCA) and DBCO-conjugated endothelial progenitor cell (EPC)-binding peptide, TPSLEQRTVYAL, (TPS-DBCO, DBCO-capped EPC-binding peptide) were clicked onto the TiO<sub>2</sub>-coated stent surface conjugated with the clickable mussel-inspired peptide using biorthogonal conjugation (Fig. 12).<sup>198</sup> The engineered stent surface had excellent inhibition of thrombosis, which may be caused by the NO-generating organoselenium site, and excellent promotion of EPC recruitment and proliferation, which may be due to the EPC-binding peptide on the engineered stent surface.<sup>198</sup> These results are interesting; however, some skill of organic synthesis is necessary

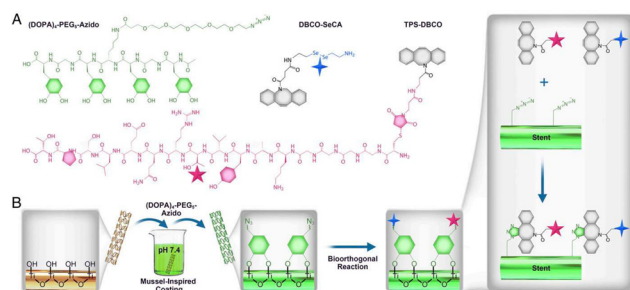


**Fig. 12** Clickable mussel-inspired peptides conjugated on titanium oxide-coated stainless stent surface using mussel-inspired adhesion. (A) Chemical scheme of the clickable mussel-inspired peptide ((DOPA)<sub>4</sub>-PEG5-Azide), NO-generating organoselenium ((DBCO)-SeCA) and RPC-binding peptide (TPS-DBCO). (B) Surface cografting on representative vascular stents through mussel-inspired coordinative interactions and biorthogonal click chemistry. Copyright 2020. Adapted with permission from PNAS. Reproduced from ref. 198 under a Creative Commons Attribution.

to prepare (DOPA)<sub>4</sub>-PEG5-azide, dibenzylcyclooctyne (DBCO)-SeCA and TPS-DBCO and apply the design to other biomaterials.

Tatrai *et al.* synthesized a branched polymer of poly[Lys(Ser<sub>0.9</sub>-DL-Ala<sub>2.7</sub>)] grafted with cyclic RGD (Fig. 13),<sup>185</sup> which could be coated on TCP dishes and titanium alloy used for surgical implants and natural bone substitutes, termed “Bio-Oss”, used in dental clinics. Human ADSCs could adhere to and proliferate on the cyclic peptide-grafted polymer-coated surface efficiently and extensively differentiated into osteoblasts on the coated surface in the differentiation medium.<sup>185</sup> To thoroughly evaluate the effect of cyclic RGD, a branched polymer of poly[Lys(Ser<sub>0.9</sub>-DL-Ala<sub>2.7</sub>)] grafted with not only cyclic RGD (cyclo(RGDfC)) peptide but also linear RGD peptide such as RGD, RGDS, and RGDSP should be synthesized. However, the usage of a coating peptide material containing cyclic RGD peptide is expected to enhance cell attachment, proliferation and differentiation of the stem cells.

**3.1.5. Genetically or chemically modified peptides conjugated to proteins as coating materials.** Peptides are genetically or chemically conjugated to proteins, and peptide-conjugated proteins can be used as coating materials.

Hayashi *et al.* prepared peptide-conjugated bovine serum albumin (BSA) as a coating material where peptides were derived from laminin-111 sequences (AG73, RKRLQVLSIRT; C16, KAFDITYVRLKF; A99, AGTFALRGDNPQG; AG10, NRWH-SIYTFRFG; and EF1XmR, RLQLQEGRLHFXFD, where X = Nle) and the thiol-maleimide click reaction was used for the conjugation of peptides and BSA (the reaction is discussed in more detail in the following section).<sup>89</sup> NPSCs can efficiently differentiate into neurons and astrocytes on TCP dishes coated with AG73 or C16 peptide-conjugated BSA. In particular, TCP dishes coated with C16 peptide-conjugated BSA facilitated the

expression of neuronal markers, such as syntaxin 1A and synaptosomal-associated protein-25.<sup>89</sup>

**3.1.6. Polydopamine as a coating support for peptide immobilization.** Mussels secrete *Mytilus edulis* foot protein-5,<sup>199,200</sup> which is an adhesive pad containing 3,4-dihydroxy-L-phenylalanine (a precursor of dopamine) and provides strong mussel adhesion on most material surfaces, including metals and organic or inorganic materials.<sup>201,202</sup> Inspired by mussels, several researchers used polydopamine for coating material surfaces.<sup>132,160,180,201,203</sup> Polydopamine-coated surfaces can adsorb bioactive peptides<sup>160,180</sup> and functional polymers such as carboxymethyl chitosan,<sup>132</sup> which can conjugate bioactive peptides using chemical reactions. When peptides contain cysteine, the cysteine thiol group can bind to the catechol group of polydopamine (Michael addition).<sup>201</sup> Furthermore, peptides contain ε-amines, such as lysine side chains, and amine groups can also conjugate to the catechol group of polydopamine.<sup>201,203</sup>

### 3.2. Chemical reaction for the immobilization of peptides

Several methods have been developed for the chemical immobilization of bioactive peptides on cell culture materials such as culture dishes, polymeric films, scaffolds, nanofibers, and hydrogels. In this case, the use of toxic materials should be avoided, especially heavy metal catalysts or organic solvents with high boiling points. This is because trace amounts of toxic heavy metals and organic solvents might remain in the final product of the cell culture materials, which would be harmful to the cells in both research and clinical application. The immobilization of peptides on cell culture materials would preferably be performed in aqueous environments or in ethyl alcohol; thus, the selection of the solvent in the reaction is very limited and would typically be aqueous solutions such as buffer solutions.

#### 3.2.1. Linker of peptides to generate functional peptides.

Peptides have amino groups and carboxylic acids on each end of peptides. Furthermore, a thiol group (–SH) can be easily introduced with the addition of cysteine to bioactive peptides. Other functional groups, such as vinyl groups, can also be introduced using linker molecules, such as 2-isocyanatoethyl methacrylate, acryloyl chloride,<sup>204</sup> acryloyl-PEG-*N*-hydroxysuccinimide (acryloyl-PEG-NHS)<sup>205</sup> and glycidyl methacrylate. Fig. 14 shows the chemical schemes of some crosslinkers to introduce functional groups on the biomolecules. 2-Isocyanatoethyl methacrylate (NCO-methacrylate) can react with the amino groups of peptides, which generates methacrylated peptides. Jia *et al.* developed a microarray of peptide-functionalized hydrogels by copolymerization of several types of methacrylated peptides and poly(ethylene glycol) diacrylate (PEGDA) with UV light irradiation.<sup>88</sup>

Glycidyl methacrylate (GMA) is typically used to introduce epoxy functional groups on material surfaces (Fig. 14). Higuchi *et al.* polymerized GMA on PS dishes or polyurethane foaming membranes where the epoxy group was generated on the surface of the dishes and membranes.<sup>206–208</sup> Subsequently, the amine group or peptide could be conjugated on the surface

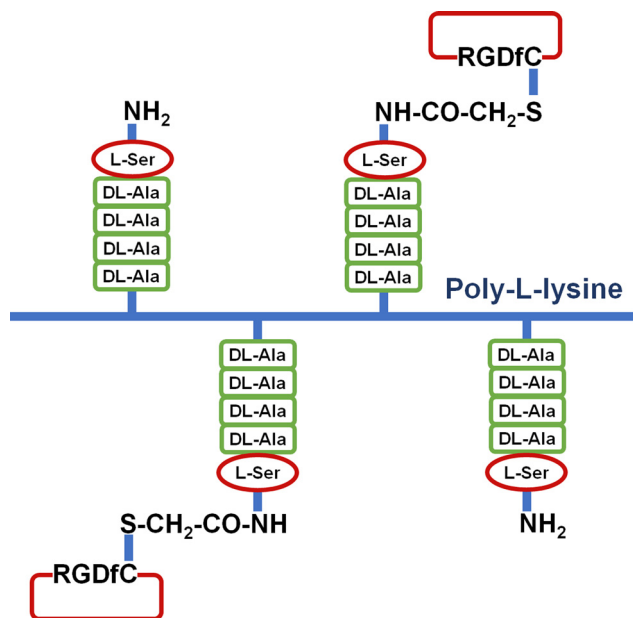
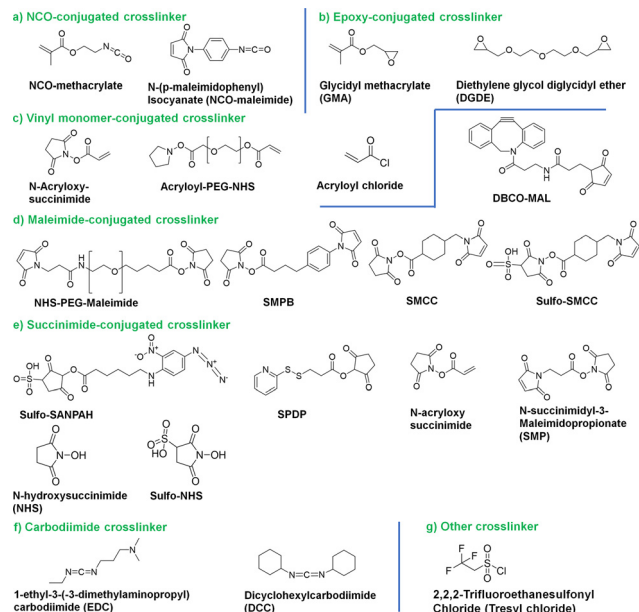


Fig. 13 Schematic scheme of a branched polymer of poly[Lys(Ser<sub>0.9</sub>-DL-Ala<sub>2.7</sub>)] grafted with cyclic RGD.



**Fig. 14** Chemical scheme of crosslinkers. (a) NCO-conjugated crosslinker (NCO-methacrylate, NCO-maleimide), (b) epoxy-conjugated crosslinker (GMA, DGDE), (c) vinyl monomer-conjugated crosslinker (*N*-acryloxysuccinimide, acryloyl-PEG-NHS, acryloyl chloride), (d) maleimide-conjugated crosslinker (NHS-PEG-maleimide, SMPB, SMCC, sulfo-SMCC and DBCO-MAL), (e) succinimide-conjugated crosslinker (sulfo-SANPAH, NHS, sulfo-NHS, SPDP, *N*-acryloxysuccinimide and SMP), (f) carbodiimide crosslinker (EDC, DCC), and (g) tresyl chloride crosslinker.

with the reaction of the deoxy group and ammonia or amine group of the peptide (CS1, EILDVPST) in aqueous solution for human hematopoietic stem cell (HSC) culture.<sup>209</sup> Furthermore, methacrylated peptides can be prepared by reacting the amino groups of peptides and GMA.

Epoxy groups can also be introduced using diethylene glycol diglycidyl ether (DGDE) (Fig. 14), which has epoxy groups on both ends and can react with a variety of functional groups.<sup>210</sup> However, DGDE has the same reactive epoxy group on both ends. Subsequently, there is the possibility of a reaction occurring between two groups on the material surface or between peptides. The reaction using DGDE contains several side reactions. Therefore, it is not generally recommended to use DGDE to conjugate material surfaces and peptides.

The primary amine of peptides can also react with acryloyl chloride in dry alcohol, which generates acrylated peptides (Fig. 14). Gao *et al.* printed acrylated peptides (GRGDS and GCRDGPQGIWQDRCG [MMP-sensitive peptide]) and PEGDA using inkjet printing (bioprinting) for bone and cartilage tissue formation with hMSCs.<sup>204</sup> Similar to acryloyl chloride, the primary amine of peptides can react with *N*-acryloxysuccinimide (Fig. 14) in *N,N*-dimethylformamide (DMF) to generate acrylated peptides.<sup>211</sup>

The azide group can be introduced on the peptide using sulfosuccinimidyl-6-[4'-azido-2'-nitrophenylamino]hexanoate (sulfo-SANPAH) in aqueous solution (Fig. 14).<sup>212,213</sup> Azide groups on peptides can react with amino groups or alkenes (vinyl groups) on material surfaces or biomolecules (Fig. 14).

Furthermore, the amine group of the peptides can be reacted with NHS-PEG-maleimide (Fig. 14) to introduce a maleimide group on the peptide. The maleimide group can further react with the thiol group on the materials (maleimide-thiol reaction). Succinimidyl-4-(*p*-maleimidophenyl)butylate (SMPB) is similar to NHS-PEG-maleimide, but phenylbutylate is introduced between NHS and maleimide instead of a flexible and biocompatible PEG segment (Fig. 14). *N*-Succinimidyl-3-maleimidopropionate (SMP) also has NHS and maleimide on each of its ends (Fig. 14), which can be used in DMF.<sup>214</sup>

*N*-(*p*-maleimidophenyl)isocyanate (PMPI, NCO-maleimide) has isocyanate on one end and a maleimide group on the other end (Fig. 14). PMPI can react with the hydroxy end group of PEG on the block copolymer of PS and PEG in DMF to introduce a maleimide group on the copolymer.<sup>215</sup> Subsequently, cysteine-containing peptides were conjugated using a maleimide-thiol reaction (Michael-type addition).

Maleimide groups can also be introduced on peptides using maleimidopropionic acid from a conjugation of primary amine and propionic acid in dichloromethane by carbodiimide chemistry.<sup>216</sup>

PEG-succinimidyl 3-(2-pyridylthio)propionate (PEG-SPDP), typically PEG4-SPDP and PEG12-SPDP, and *N*-succinimidyl-3-(2-pyridylthio) propionate (SPDP)<sup>217</sup> work similarly to NHS-PEG-maleimide. PEG-SPDP (used in aqueous solution) and SPDP (used in DMF or dimethyl sulfoxide (DMSO)) (Fig. 14) react with the amine group of the peptides and can introduce a sulfhydryl-reactive 2-pyridylthio group, which can bind to cysteine-containing peptides or thiol group-conjugated materials and molecules.

Dibenzylcyclooctyne-maleimide (DBCO-MAL) (Fig. 14) efficiently incorporates DBCO groups onto cysteine-containing peptides and material surfaces or other thiol-containing molecules and material surfaces.<sup>198</sup> The maleimide group reacts with sulfhydryl (thiol) groups such as cysteine to form stable thioether bonds. DBCO can conjugate with an azide group, which does not require cytotoxic Cu(I) catalyst (copper-free click reaction).

$N_3$ -PEG<sub>5</sub>-COOH can introduce azido groups on peptides or material surfaces.<sup>198</sup> For example, the primary amine can be conjugated with the carboxylic acid of  $N_3$ -PEG<sub>5</sub>COOH using carbodiimide chemistry in aqueous solution.

The above reaction can also be used on the material surface to introduce functional groups on the materials. Typically, the material surfaces are activated by introducing NHS-PEG-maleimide, SMPB, PEG-SPDP, sulfo-SANPAH, and cysteine-introduced peptide on the activated material surface (thiol-ene reaction).<sup>218</sup> Most researchers use NHS-PEG-maleimide in the thiol-ene reaction.<sup>219,220</sup> These reactions can be performed in aqueous solution. Therefore, these reactions are nontoxic and do not damage the peptides and material surfaces in general.

Maleimide-streptavidin can introduce cysteine-conjugated peptides or thiol-containing materials using a maleimide-thiol reaction (Michael-type addition). Furthermore, biotinylation of the peptides or materials can be performed using a biotin-protein ligase kit in aqueous solution.<sup>221</sup> Biotin-avidin



(streptavidin) binding can contribute to the conjugation of peptides on the material surface.

2,2,2-Trifluoroethanesulfonyl chloride (tresyl chloride) (Fig. 14) can react with hydroxy groups, such as glass plates, and introduce a tresyl group.<sup>222,223</sup> The activated surface can react with the primary amine of the peptides, where the peptides are covalently bonded on the material surface with hydroxy groups.

**3.2.2. Reaction between functional groups of the material surface and peptides.** Peptides can be conjugated on material surfaces such as plastic dishes, polymeric films, scaffolds, nanofibers and hydrogels by the reaction of functional groups between the peptides and surfaces. There are several combinations of functional group reactions between peptides and the material surfaces, and they are summarized in Fig. 15. Peptides have amino groups (a) and carboxylic acids (b) on each end. Furthermore, a sulfhydryl (thiol) group (–SH) (c) can be introduced with the addition of cysteine to the bioactive peptides given in Fig. 15, as discussed in the previous section. An alkene (vinyl group) (d) can be introduced using acryloyl chloride, 2-isocyanatoethyl methacrylate and GMA as described in the previous section. A hydroxy group (e) can be introduced with the addition of serine, threonine, and tyrosine on the bioactive peptides. The maleimide group (f) can be introduced using NHS-PEG-maleimide, SMPB, SMCC and sulfo-SMCC (Fig. 14). An azide group (g) can be introduced on the peptide using sulfo-SANPAH and N3-PEG5-COOH as described in the previous section (Fig. 15).

Biodegradable polymers that can be conjugated with bioactive peptides and used for stem cell culture and differentiation include poly-L-lactide (PLLA), PLGA, chitosan, carboxymethyl chitosan, alginate, hyaluronic acid (HyA), polycaprolactone (PCL) and poly-(3-hydroxybutyrate-co-3-hydroxyvalerate); these polymers can be used to generate nanofibers, scaffolds and hydrogels (Fig. 8). Nonbiodegradable polymers, such as PS, poly(*N*-isopropylacrylamide), polyhydroxyethylmethacrylate (polyHEMA), polyacrylate, polyacrylamide and polyurethane, are also used as polymeric films, dishes, scaffolds and hydrogels for stem cell culture and differentiation (Fig. 8). These material surfaces may or

may not have functional groups to react with peptides. When the material surface does not have appropriate functional groups, the functional groups are introduced by physical treatment, such as ozone treatment from  $\gamma$ -ray irradiation and plasma treatment, or chemical treatment, such as hydrolysis. Copolymerization with a small portion of monomer-containing functional side chains is also useful for the preparation of synthetic materials. When the materials have some functional groups, such as hydroxy groups, carboxylic acid groups or amino groups, a variety of other functional groups, such as alkene (vinyl) groups, alkynes, sulfhydryl (thiol) groups, epoxy groups, isocyanate groups, azido groups, and maleimide groups, can be introduced using reactions similar to those described above.

In the following sections, the reaction among these functional groups on peptides and material surfaces (biomolecules) will be discussed in more detail. Fig. 16 shows the summary of reactions of bioactive peptides grafted onto a material surface using several different reaction methods. Fig. 17 shows the probabilities of each grafting reaction on the grafting of peptides on the biomaterials; this information is summarized in Table S10 (ESI†).

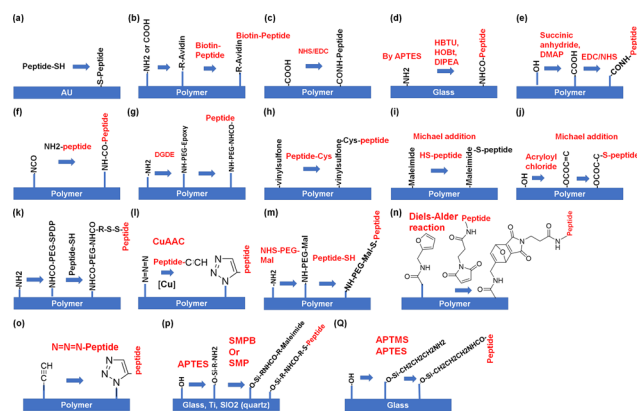


Fig. 16 Schematic illustration of several reactions of peptides grafted onto biomaterials. (a) Gold–sulfur reaction (sulfhydryl peptide reaction on gold-coated biomaterials). (b) Avidin–biotin reaction (biotinylated peptide reaction on avidin-immobilized biomaterials). (c) Carbodiimide reaction. (d) Reaction of the amine group on glass with the carboxylic acid group of peptides using HBTU, HOBt or DIPEA. (e) Reaction of hydroxy groups on biomaterials with amine groups of peptides using succinic anhydride or DMAP and EDC/NHS. (f) Reaction of isocyanate-conjugated biomaterials with amine groups of peptides. (g) Reaction of amine groups on biomaterials with amine groups of peptides using DGDE. (h) Reaction of vinylsulfone-conjugated biomaterials with sulfhydryl peptides. (i) Michael-type addition reaction (reaction of maleimide-conjugated biomaterials with sulfhydryl peptides). (j) Michael-type addition reaction (reaction of hydroxyoxide group-conjugated biomaterials with sulfhydryl peptides using acryloyl chloride). (k) Reaction of amine groups on biomaterials with sulfhydryl peptides using PEG-SPDP. (l) CuAAC click reaction (azide-conjugated biomaterials with alkyne-conjugated peptides and a copper(i) catalyst). (m) Reaction of amine groups on biomaterials with sulfhydryl peptides using NHS-PEG-maleimide. (n) Diels–Alder reaction. (o) Reaction of alkyne groups on biomaterials with azide-conjugated peptides. (p) Reaction of hydroxy groups on biomaterials with sulfhydryl peptides using SMPB or SMP. (q) Reaction of hydroxy groups on glass with peptides using APTMS or APTES.

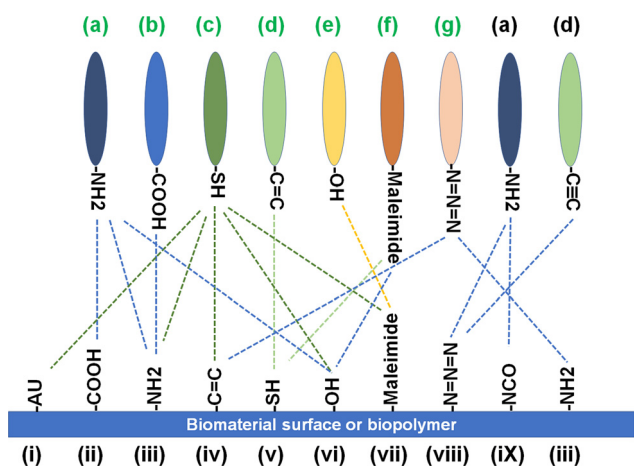


Fig. 15 Reaction combination among functional groups located on peptides and biomaterial or biopolymer surface.



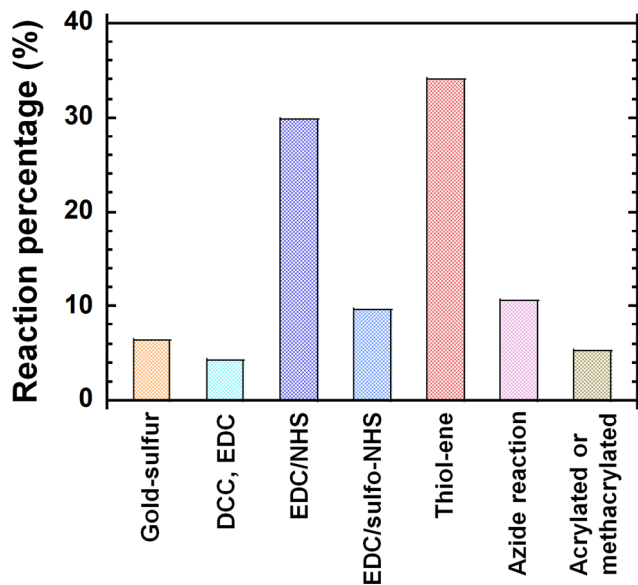


Fig. 17 Percentage of each reaction for peptide-grafting on biomaterials analyzed from the literature from January 2010 to April 2022.

### 3.2.3. Specific reaction between functional groups of material surface and peptides

**3.2.3.1. Gold-sulfur group reaction.** When the peptides have sulfhydryl (thiol) groups, the peptides can directly react on the gold surface (gold-sulfur reaction) (Fig. 16). Gold can be coated on the surfaces of glass coverslips, ITO electrodes and polymeric films, nanofibers or scaffolds using Pd-Au sputtering, which is typically used for scanning electron microscopy (SEM) measurements. To generate a gold-coated surface grafted with peptides, the gold-coated surface is immersed in aqueous alkanethiol solutions, which can be conjugated with bioactive peptides to generate SAMs,<sup>91,224–228</sup> or the gold-coated surface is immersed with aqueous cysteine-containing peptide solution.<sup>1,229–231</sup>

**3.2.3.2. Carbodiimide reaction.** The amino (primary amine) groups (or carboxylic acids) of peptides can react with carboxylic acids (or amino (primary amine) groups) on the material surface or biomacromolecules using the *N*-hydroxysuccinimide (NHS)/1-ethyl-3-(3-dimethylaminopropyl) carbodiimide hydrochloride (EDC) reaction (Fig. 16)<sup>68,93–95,105,109,131,132,159–164,168,232–240</sup> or the NHS/*N*-hydroxysulfosuccinimide (sulfo-NHS) reaction (Fig. 16).<sup>124,133,241–247</sup> Because most natural or synthetic materials can originally have or easily introduce amine or carboxylic acid functional groups, the carbodiimide reaction is one of the most popular reactions for the introduction of peptides on materials (Fig. 17).

The expected reaction scheme of EDC/NHS and EDC/sulfo-NHS chemistry is shown in Fig. 18. Carbodiimidazole (CDI)<sup>104</sup> and dicyclohexylcarbodiimide (DCC)<sup>165,248,249</sup> can work similarly to EDC. However, the EDC reaction with and without NHS or sulfo-NHS is a popular reaction for the conjugation between the primary amine and carboxylic acid. EDC and carbodiimide can conjugate carboxylic acid with only the primary amine group,<sup>250</sup> but the addition of NHS or sulfo-NHS into the EDC reaction

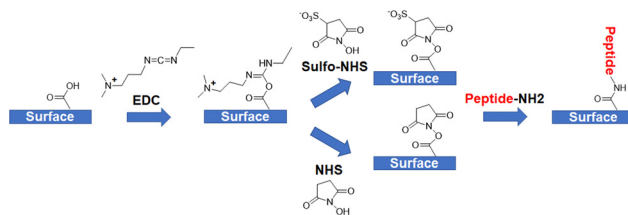


Fig. 18 Carbodiimide reaction scheme using EDC/NHS and EDC/sulfo-NHS for peptide grafting on biomaterials containing carboxylic acid.

solution enhances the reaction efficiency. Therefore, most recent studies have used EDC together with NHS or sulfo-NHS to conjugate peptides on material surfaces or biomacromolecules. Among studies published from January 2010 to April 2022 using immobilization reactions of bioactive peptides on materials, 30% used the EDC/NHS reaction, 10% used the EDC/sulfo-NHS reaction, and only 4% used EDC (previously called water soluble carbodiimide) or DCC only (see Fig. 17 and Table S10, ESI<sup>†</sup>). Because this reaction can be performed in aqueous solution, it is one of the most common reactions to graft peptides on material surfaces or biomacromolecules.

**3.2.3.3. Thiol-ene reaction including the maleimide-thiol reaction (Michael-type addition).** The carbodiimide reaction is one of the most popular reactions to conjugate peptides on materials, and the next most popular reaction is the thiol-ene reaction, including the maleimide-thiol reaction<sup>251,252</sup> (Fig. 16 and 19). This reaction is also called Michael-type addition or the click reaction<sup>253,254</sup> and is mainly performed in aqueous solution. Maleimide can be introduced onto material surfaces or peptides using the crosslinker NHS-PEG-maleimide or SMPB, which can connect maleimide groups to the peptides or to material surfaces that have primary amines. SPDP and PEG-SPDP (typically PEG4-SPDP (spacer arm length = 25.7 angstroms) and PEG12-SPDP (spacer arm length = 54 angstroms)) can introduce pyridyldithiol, which can conjugate with cysteine-containing peptides or material surfaces having thiol groups (Fig. 19), as described in the previous section.

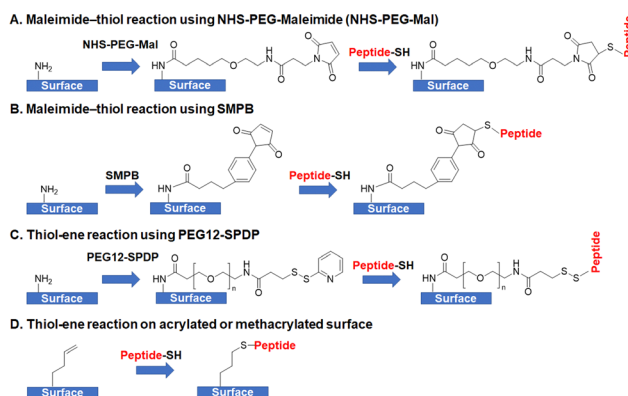


Fig. 19 Thiol-ene reaction (Michael-type addition) for grafting of sulfhydryl peptides (A–C) onto biomaterials conjugated with amine groups using (A) NHS-PEG-maleimide, (B) SMPB and (C) PEG12-SPDP and (D) on acrylated or methacrylated biomaterials.

Acrylated or methacrylated hydrogels can be prepared using copolymerization of acrylated or methacrylated monomers such as poly(ethylene glycol) tetraacrylate (PEGTA),<sup>1,255</sup> PEGDA,<sup>256</sup> poly(ethylene glycol) dimethacrylate (PEGDM),<sup>126</sup> and methacrylic anhydride.<sup>257</sup> Song *et al.* prepared acrylated HyA using acryloxy-succinimide (Fig. 14).<sup>258</sup> Jiang *et al.* used vinylsulfone-functionalized poly(vinyl alcohol) hydrogels (Fig. 8).<sup>150</sup> Acrylated poly(L-lactide) (PLL) or poly(lactic-co-glycolic acid) (PLGA), can be prepared by partial hydrolysis of these biodegradable polyesters and subsequent reaction with acryloyl chloride.<sup>130</sup> The polymerization can be performed by photoirradiation, radical polymerization<sup>126</sup> or multithiol molecules such as PEG dithiol<sup>255</sup> and four-arm thiolated PEG.<sup>1</sup>

Then, an aqueous solution of the peptides containing cysteine (where cysteine is typically added on the N end of the peptides) is added into the acrylated or methacrylated hydrogels or polymers for the conjugation of peptides on the hydrogels using the thiol-ene reaction (Michael-type addition) (Fig. 19). This reaction is also called the click reaction and is highly efficient. Dhillon *et al.* also conjugated the IKVAV peptide (CSRARKQAASIKVAVSADR) on *N*-methacrylate glycol chitosan hydrogels using a thiol-ene reaction.<sup>211</sup> Park *et al.* prepared the BMP peptide KIPKASSVPTLSAISTLYL, where a cysteamide residue (-SH) was conjugated and the BMP peptide was conjugated to gelatin methacrylate using a thiol-ene reaction.<sup>259</sup> Several other studies have also demonstrated peptide-conjugated materials using a thiol-ene reaction.<sup>128,255,260</sup>

Bilem *et al.* conjugated the BMP-2 (CKIPKASSVPTLSAISMLYL) peptide and RGD (CG-K(PEG3-TAMRA (5-carboxytetramethylrhodamine))-GGRGDS) peptide on borosilicate glass slides using the following process.<sup>261,262</sup> The glass slides were aminated by treatment with 3-aminopropyltriethoxysilane (APTES) solution. Then, the aminated glass surface was treated with SMPB solution (Fig. 14) for the conjugation of the maleimide group on the glass slide. Subsequently, maleimide-functionalized glass slides were immersed in cysteine-containing peptides to conjugate peptides onto the glass slides.<sup>261,262</sup>

Seidlits *et al.* prepared thiolated HyA hydrogels from 4-arm PEG-maleimide and thiolated HyA, which were prepared from cystamine conjugation on HyA using carbodiimide chemistry, by Michael-type addition (maleimide-thiol reaction).<sup>90</sup> Before gelation of the hydrogels, cysteine-containing peptides (GCGYGRGDS, GCGYGIKVAADR and GCGYGIYSR) were added to the solution to generate peptide-conjugated HyA hydrogels.<sup>90</sup>

Li *et al.* prepared maleimide-functionalized poly(carbonate ester) by copolymerization of furan-maleimide-functionalized trimethylene carbonate and L-lactide, and subsequently, maleimide-functionalized poly(carbonate ester) was obtained by the retro Diels-Alder reaction<sup>263,264</sup> (Fig. 16) of furan-maleimide-functionalized poly(carbonate ester).<sup>265</sup> The cysteine-conjugated peptide CEPLQLKM (E7, BMSC affinity peptide) was added and conjugated to the maleimide-functionalized poly(carbonate ester) in DMF solution using the maleimide-thiol reaction (Michael-type addition).

Ratcliffe *et al.* used maleimide-conjugated cyclo-arginine-glycine-aspartate (c-RGD) for the conjugation of c-RGD to

the thiol group of thiol-acrylate emulsion-templated porous polymers.<sup>266</sup>

Several other researchers also used maleimide-functionalized materials (or peptides) to conjugate cysteine-conjugated peptides (or thiol-containing materials) using a maleimide-thiol reaction (Michael-type addition).<sup>117,214,215,267,268</sup>

**3.2.3.4. Acrylated or methacrylated peptide reaction.** Acrylated or methacrylated hydrogels can be prepared using copolymerization of acrylated or methacrylated monomers such as PEGTA,<sup>1,255</sup> PEGDA,<sup>256</sup> PEGDM,<sup>126</sup> and methacrylic anhydride,<sup>257</sup> as discussed in the previous section. Acrylated or methacrylated peptides can also be prepared using acryloyl chloride, methacryloyl chloride, *N*-acryloxysuccinimide, *N*-(methacryloyloxy)succinimide, and acryloyl-PEG-NHS (Fig. 14), as discussed in the previous section. Then, acrylated or methacrylated monomers and peptides can be copolymerized to generate peptide-conjugated hydrogels.

Jia *et al.* prepared methacrylated peptides using methacryloyl chloride and made peptide-functionalized hydrogels by copolymerization of several types of methacrylated peptides and PEDGA.<sup>87,88</sup> Similar peptide-functionalized hydrogels have been prepared in several other studies using different types of monomer-conjugated or unconjugated peptides.<sup>204,205,211</sup>

**3.2.3.5. Azide reaction.** Several reactions using azide groups can be used to conjugate bioactive peptides on biomaterials, such as (a) azide-amine reactions<sup>212,213,269</sup> and (b) azide-alkyne reactions, including copper(i)-catalyzed azide-alkyne cycloaddition (CuAAC)<sup>227,270-272</sup> and strain-promoted alkyne-azide cycloaddition (SPAAC) reactions.<sup>273-276</sup> Two examples of SPAAC reactions are azide-DBCO reactions<sup>99,100,198,201</sup> and azide-dibenzocyclooctynol (azide-DIBO) reactions<sup>277</sup> (Fig. 14, 16 and 20). These azide reactions will be discussed in more detail in the following sections.

**3.2.3.5.1. Azide-amine reaction.** Azide groups can be introduced on the peptide or material surface using sulfo-SANPAH

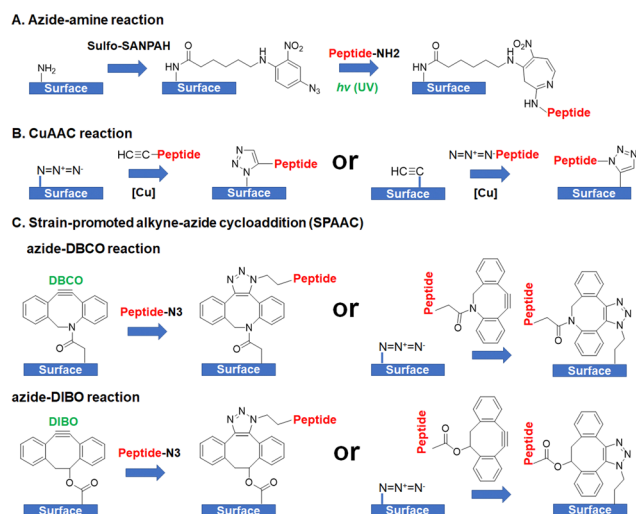


Fig. 20 Azide reaction (Michael-type addition) for grafting peptides onto biomaterials. (A) Azide-amine reaction using sulfoSANPAH. (B) Azide-alkyne (CuAAC) reaction. (C) SPAAC reaction using DBCO or DIBO and azide functional groups.

(Fig. 20(A)).<sup>212,213</sup> Azide groups on peptide or material surfaces can react with amino groups or alkenes (vinyl groups) on material surfaces or biomolecules such as peptides. Qin *et al.* prepared *N*-cadherin mimetic peptide (HAVDIGGGK)-conjugated polyacrylamide hydrogels using sulfo-SANPAH, where sulfo-SANPAH solution was added to the polyacrylamide hydrogels to introduce azide groups on the hydrogels (Fig. 20(A)).<sup>212</sup> Subsequently, the acrylamide hydrogels were exposed to UV light for 8 min, and the *N*-cadherin mimetic peptide solution was added to the hydrogels to be conjugated with the peptide.

**3.2.3.5.2. CuAAC reaction.** 1,3-Dipolar cycloaddition is the copper(i)-catalyzed variant of the azide-amine reaction, in which organic azides and terminal alkynes are conjugated to generate 1,4-regioisomers of 1,2,3-triazoles. This reaction is called copper(i)-catalyzed azide-alkyne cycloaddition (CuAAC).<sup>278</sup>

In several studies, bioactive peptides have been conjugated to biomaterials using the CuAAC reaction (Fig. 20(B) and Table S10, ESI†).<sup>227,270</sup> Hudalla and Murphy prepared SAMs on a gold surface where azide-terminated hexaethylene glycol alkanethiolates and carboxylic acid-terminated hexaethylene glycol alkanethiolates were conjugated using a Au-sulfur reaction.<sup>227</sup> Using NHS/EDC chemistry, TYRSRKY, which is a heparin sulfate proteoglycan-mediated adhesion peptide for hBMSCs, was conjugated to carboxylic acid-terminated hexaethylene glycol alkanethiolates, whereas acetylene-conjugated RGDS was conjugated to azide-terminated hexaethylene glycol alkanethiolates in a solution containing CuBr, sodium ascorbate and tris[(1-benzyl-1*H*-1,2,3-triazol-4-yl)methyl]amine (TBTA) using the CuAAC click reaction (Fig. 20(B)).<sup>227</sup> In the study, two different types of bioactive peptides, TYRSRKY and RGDS, were conjugated on the terminated side of alkanethiolates.

Dvorakova *et al.* designed injectable hydrogels based on poly( $\alpha$ -amino acid)s conjugated with a bioactive peptide (RGDSGGGY).<sup>270</sup> First, poly( $N^{\epsilon}$ -(2-hydroxyethyl)-L-glutamine) derivatives with tyramine units (PHEG-Tyr) were prepared. Then, azidoacetic-(CH<sub>2</sub>-CH<sub>2</sub>O)<sub>6</sub>RGDSGGGY-NH<sub>2</sub> was conjugated on the propargylated units of PHEG-Tyr from the CuAAC click reaction (Fig. 20(B)) in a solution containing sodium ascorbate and the Cu-THPTA complex.<sup>270</sup> One of the drawbacks of the CuAAC reaction is that the Cu catalyst might contaminate the final product of the reaction.

**3.2.3.5.3. Azide-alkyne cycloaddition (SPAAC) reaction.** Rong *et al.* prepared poly(L-glutamic acid) (PLG) hydrogels grafted with cyclic RGD (cyclo(RGDfK)) and an *N*-cadherin mimetic peptide (HAVDIGGGK) using azide-alkyne cycloaddition (SPAAC) between azidobenzocyclooctyne-grafted PLG and azido-grafted PLG. Azidobenzocyclooctyne-grafted PLG was prepared using the reaction between the carboxylic acid of PLG and the primary amine group of azidobenzocyclooctyne-ethylamine by EDC/NHS chemistry. Azido-grafted PLG was synthesized from the conjugation of PLG with 2-(2-azidoethoxy)ethanol using the EDC/4-dimethylaminopyridine (DMAP)-mediated coupling reaction. Azido-grafted PLG conjugating cyclic RGD and the *N*-cadherin mimetic peptide was prepared using the NHS/EDC

reaction between the carboxylic acid of PLG and the primary amine of the bioactive peptides.<sup>273</sup>

**3.2.3.5.4. SPAAC reaction using the azide-DBCO reaction.** Perera *et al.* conjugated dual laminin-derived peptides (LREGGGC and GIKVAV) on HyA hydrogels using a thiol-ene reaction and azide-alkyne cycloaddition. First, a thiol functional group was introduced to HyA by reaction with dithiothreitol and ethylene sulfide.<sup>99,100</sup> Subsequently, thiol-functionalized HyA was grafted with azide functional groups by reaction with 11-azido-3,6,9-trioxaundecan-1-amine using EDC/NHS chemistry. LREGGGC was reacted with dibenzocyclooctyne (DBCO)-maleimide from the maleimide-thiol reaction, which introduced a DBCO functional group onto LREGGGC. Then, the DBCO functional group on DBCO-LREGGGC was reacted with the azide group on thiol- and azide-functionalized HyA (Fig. 20(C)).<sup>99,100</sup> Then, the thiol group on thiol- and azide-functionalized HyA was reacted with acrylated GIKVAV, which was synthesized from the reaction of GIKVAV with acryloyl chloride. Finally, LREGGGC- and GIKVAV-conjugated HyA were prepared for neurite extension of hiPSC-derived neural stem cells<sup>100</sup> and mouse ESCs.<sup>99</sup>

**3.2.3.5.5. SPAAC reaction using the azide-DIBO reaction.** Callahan *et al.* prepared aligned and random polylactide (PLLA) nanofibers conjugated with GYIGSR (a laminin-derived peptide) using metal-free click chemistry where DIBO is terminated on PLLA using a catalyst of 1,8-diazabicyclo[5.4.0]undec-7-ene (Fig. 20(C)).<sup>277</sup> The azide-substituted peptide was reacted with the triple bond of DIBO on DIBO-conjugated PLLA to generate GYIGSR-conjugated PLLA (Fig. 20(C)), which was electrospun to make aligned or random nanofibers<sup>2,4,279-281</sup> for the culture and differentiation of mouse ESCs.<sup>277</sup>

**3.2.3.6. Diels-Alder reaction.** The Diels-Alder reaction is used to form a substituted cyclohexene derivative from the reaction of a conjugated diene with a substituted alkene (dienophile) (Fig. 21(A)). Silva *et al.* used the Diels-Alder reaction to prepare GRGDS peptide-conjugated gellan gum hydrogels where furan-

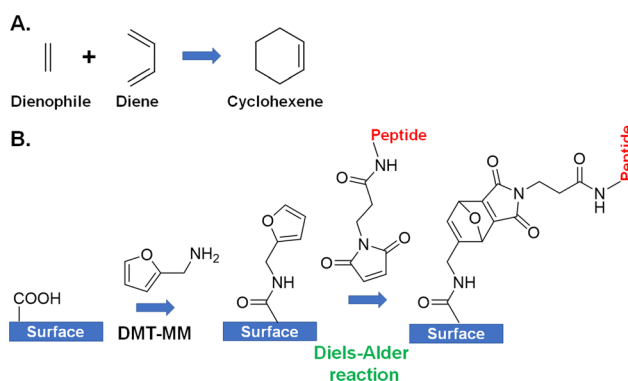


Fig. 21 Diels-Alder reaction for grafting peptides onto biomaterials. (A) The Diels-Alder reaction generated to form a substituted cyclohexene derivative from the reaction of a conjugated diene with a substituted alkene (dienophile). (B) Peptide-conjugated hydrogels where the furan-conjugated surface was reacted with maleimide-conjugated peptide.



conjugated gellan gum was reacted with maleimide-conjugated peptide (Fig. 21(B)).<sup>216</sup>

### 3.3. Design of peptides with a joint chain and a dual chain

Higuchi *et al.* developed several bioactive peptide-grafted poly(vinyl alcohol-co-itaconic acid) (PVA-IA) hydrogels, which have optimal elasticity for hPSC culture (25 kPa in the study).<sup>161</sup> The peptides used in the study were derived from BSP (BSP-1, KGGNGEPRGDTYRAY), heparin binding protein (HBP-1, GKKQRFHRNRKKG; HBP-2C, CGGGKQRFHRNRKKG), and vitronectin (VN-1, KGGPQVTRGDVFTMP; VN-4G, GGGGKGGPQVTRGDVFTMP; VN-2C, GCGGKGGPQVTRGDVFTMP), where the VN-1 peptide is the only bioactive peptide, VN-4G and VN-2C added a joint segment of GGGG and GCGG, respectively, and VN-2C contains cysteine, which contributes to a dual chain.<sup>161</sup> HBP-2C also contains cysteine and joint segments, whereas HBP-1 does not. They also prepared the branched type of peptide using the main chain and BOP-1 (Fig. 22). When the peptide-grafted PVA-IA hydrogels were prepared with a relatively high concentration peptide solution ( $> 500 \mu\text{g mL}^{-1}$ ), hESCs could attach to the peptide-grafted PVA-IA hydrogels. However, when the peptide-grafted PVA-IA hydrogels were prepared with a relatively low concentration of peptide ( $200 \mu\text{g mL}^{-1}$ ), hESCs did not attach and proliferate as well on the BSP-grafted PVA-IA hydrogels.

hESCs could attach to the peptide-grafted PVA-IA hydrogels in the chemically defined medium Essential 8, where the hydrogels were prepared with peptides containing the integrin-binding site RGD (BSP-1, VN-1, VN-4G, VN-2C, and BOP-1).<sup>161</sup> However, the PVA-IA hydrogels prepared with peptides of heparin-binding proteins (glycosaminoglycan, GAG, binding domain), such as HBP-1 and HBP-2C, could not support hESC adhesion and proliferation. Considering the results of Klim

*et al.*,<sup>225</sup> cell culture surfaces containing GAG binding domains could not support hPSC adhesion and proliferation without cyclic RGD peptide immobilization. hESCs cultured on the peptide-grafted PVA-IA hydrogels that have a joint segment, which are prepared from VN-4G and VN-2C, expand faster than hESCs cultured on the hydrogels prepared with a peptide without a joint segment (VN-1).<sup>161</sup> Furthermore, the peptide-grafted PVA-IA hydrogels prepared from a peptide that has a dual chain motif (VN-2C) support a higher proliferation speed of hESCs and hiPSCs than the hydrogels prepared with other peptides in chemically defined Essential 8 medium do.<sup>161</sup> Therefore, the design of peptides containing an adequate joint segment and a dual chain structure is valuable. The hESCs and hiPSCs after 10 passages of culture showed excellent pluripotent protein expression and high differentiation ability into cells derived from three germ layers *in vitro* (embryoid body formation assay) and *in vivo* (teratoma formation assay).

Jia *et al.* investigated the length of the linker (glycine numbers) between methacrylated-PEGDA hydrogels and a bioactive peptide (RGDSP).<sup>88</sup> They conjugated the peptide with (a) no glycine linker, (b) 2 glycine linkers, (c) 4 glycine linkers and (d) 6 glycine linkers. They evaluated hADSC attachment on these hydrogels. hADSCs could attach more effectively to peptide-grafted hydrogels with longer linkers, such as 4 glycine and 6 glycine, than hydrogels with zero or 2 glycine linkers.<sup>88</sup> This is because of the enhanced moving flexibility of the peptides to find integrin receptors on the cells. Furthermore, there was no significant difference in the number of hADSCs attached to peptide-grafted hydrogels with 4 glycine linkers and 6 glycine linkers.<sup>88</sup> Therefore, they concluded that 4 glycine linkers ensure sufficient exposure of peptide moieties to the cells.

## 4. Stem cell culture and differentiation on biomaterials conjugated with bioactive peptides

### 4.1. Stem cells on hydrogels conjugated with bioactive peptides

When the peptides were conjugated to methacrylated or acrylated monomers, the peptide-conjugated hydrogels can be prepared from copolymerization of hydrophilic monomers and monomer-conjugated peptides as discussed previously.

One of the most typical methods to conjugate bioactive peptides on polymeric materials is to conjugate the bioactive peptides with the carboxylic acid group of the material surface using carbodiimide reactions such as EDC/NHS chemistry (Fig. 14, 17 and 18). Higuchi *et al.* prepared PVA-IA hydrogels on TCPS dishes. Several bioactive peptides were conjugated to the PVA-IA hydrogels using EDC/NHS chemistry.<sup>68,161,164</sup> PVA-IA hydrogels grafted with a peptide derived from laminin- $\beta$ 4 (PMQKMRGDVFTMP) containing a joint segment (GGGG), dual chain motif (GCGG) and cationic amino acid insertion (KGG) facilitated hPSC attachment and promoted excellent expansion in long-term culture (over 10 passages) with low differentiation

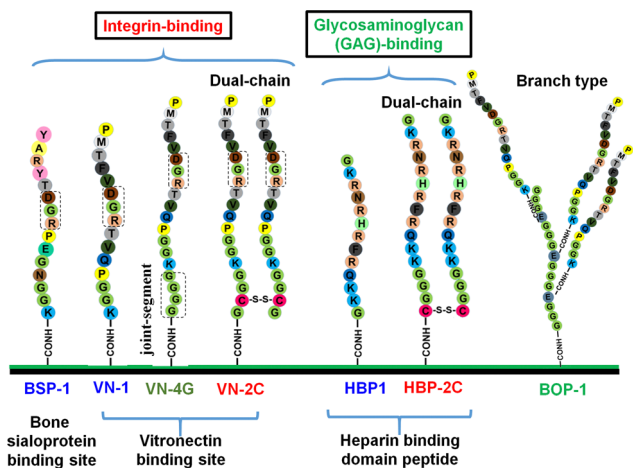


Fig. 22 Design and sequence of peptides grafted onto hydrogels. Single chains (BSP, PVA-VN1, and HBP1), single chains with a joint segment (VN-4G), dual chains (VN-2C and HBP-2C), and branch-type (BOP-1) peptides were conjugated to PVA-IA hydrogels. BSP, VN1, VN-4G, VN-2C, and BOP-1 have an integrin-binding domain, whereas HBP1 and HBP-2C have a glycosaminoglycan-binding domain. Modified from ref. 161 under a Creative Commons Attribution.



rates. However, hPSCs attached weakly to PVA-IA hydrogels conjugated with laminin- $\alpha$ 5 peptides (PASYRGDSC), which had joint segments with and without a cationic amino acid (GGGGKGGPASYRGDSC, GCGGKGGPASYRGDSC, and GGGGPA-SYRGDSC), or to PVA-IA hydrogels conjugated with laminin- $\beta$ 4 peptides containing the joint segment only. The addition of a cationic amino acid (KGG) to the laminin- $\beta$ 4 peptide (GGGGKGGPMQKMRGDFVSP and GCGGKGGPMQKMRGDFVSP) was valuable for hPSC adhesion to PVA-IA hydrogels, contributing to the zeta potential shifting to higher values (3–4 mV increase). Better hPSC proliferation was seen with the novel peptide segment-conjugated PVA-IA hydrogels facilitated than with recombinant VTN-coated plates (a well-established standard for hPSC culture) in xeno-free culture conditions. After long-term culture on peptide-grafted hydrogels, hPSCs differentiated into specific lineages of cells, such as cardiomyocytes, with extensive efficiency.

Gao *et al.* prepared an acrylated peptide using the reaction between GRGDS or MMP-sensitive peptide and acryloyl chloride.<sup>204</sup> The solution of PEGDMA, acrylated GRGDS and acrylated MMP-sensitive peptide together with a photoinitiator (I-2959) was mixed with hBMSCs, and then the PEG-peptide solution was bioprinted using a 3D bioprinting platform. hBMSCs in the PEG-peptide scaffolds extensively enhanced osteogenic and chondrogenic differentiation for bone and cartilage formation.<sup>204</sup>

The alginate (Fig. 8) solution can be solidified by the addition of divalent cations such as  $\text{Ca}^{2+}$  or  $\text{Mg}^{2+}$ . Alginate hydrogels conjugated with peptides can be prepared as follows. Jia *et al.* prepared oxidized alginate, which was conjugated with peptide by CuAAC click chemistry.<sup>87</sup> The peptide-conjugated alginate solution was injected into  $\text{Ca}^{2+}$ -containing gelatin dishes to generate peptide-conjugated alginate hydrogels. The attachment of HUVECs to peptide-conjugated alginate hydrogels was then investigated.

Simmons *et al.* prepared peptide-conjugated alginate using EDC/NHS chemistry.<sup>241</sup> The peptide-conjugated alginate, rat BMSCs, and growth factors (BMP-2 and transforming growth factor- $\beta$ 3 (TGF- $\beta$ 3)) were mixed, and the alginate-BMSC solution was cross-linked with calcium sulfate to generate hydrogels conjugated with bioactive peptides and entrapping rat BMSCs.

Luo *et al.* designed dual peptide-loaded alginate hydrogels for hMSC proliferation and differentiation,<sup>246</sup> where an RGD peptide (GGGGRGDASSP) contributes to cell adhesion and proliferation and bone forming peptide-1 (BFP-1, GQGFSYPY-KAVFSTQ) contributes to hMSC differentiation into osteoblasts. The authors prepared BFP-1-loaded mesoporous silica nanoparticles (MSNs). Then, the RGD peptide was conjugated to the carboxylic acid of alginate using EDC/Sulfo-NHS chemistry. BFP-1-loaded MSNs were mixed with RGD peptide-conjugated alginate and subsequently crosslinked to generate BFP-1-loaded MSN/RGD peptide-conjugated alginate hydrogels with a calcium sulfate slurry.<sup>246</sup> This study indicated that sequential stimulation by the RGD peptide and osteogenic induction by the BFP-1 peptide could synergistically promote cell adhesion, survival, proliferation and osteogenic differentiation compared

to the cells treated with a single peptide or simultaneous stimulation.

In several other studies,<sup>124,242–245,282,283</sup> peptide-conjugated alginate (Fig. 8) was prepared using an EDC/NHS solution (Fig. 18) or other carbodiimide reaction solutions where the peptide-conjugated alginate solution was inserted or printed on  $\text{Ca}^{2+}$ -containing gelatin film on the dishes or injected into  $\text{Ca}^{2+}$  solution, which generated peptide-conjugated hydrogels on the dishes, because the alginate solution can be crosslinked in the presence of divalent cations such as  $\text{Ca}^{2+}$ .

Salinas *et al.* prepared PEG hydrogels conjugated with bioactive peptides using a photoinitiated thiol-acrylate reaction (Fig. 19).<sup>256</sup> hBMSCs were suspended in PEGDA and the peptide together with a photoinitiator, 4-(2-hydroxyethoxy)-phenyl-(2-hydroxy-2-propyl)ketone. Subsequently, the suspension was irradiated under light at 365 nm with  $5 \text{ mW cm}^{-2}$  for 10 min at room temperature.<sup>256</sup> The hBMSCs entrapped in the PEG hydrogels conjugated with peptides having a glycine spacer (a joint segment), CGGGGGGGGRGDSG, showed a better survival rate than those in the PEG hydrogels conjugated with peptides without a glycine spacer (CRGDSG or CRGDSCG).<sup>256</sup> Although light irradiation with  $5 \text{ mW cm}^{-2}$  for 10 min is relatively strong (irradiation with a typical laser pointer of 1–5 mW) for the cells, the cells can be easily entrapped into PEG hydrogels using the photoinitiated thiol-acrylate reaction.

Nguyen *et al.* also prepared PEG hydrogels using a thiol-ene reaction. Twenty kilodalton 8-arm PEG-norbornene was prepared from the reaction of 8-arm PEG-OH and norbornene using a carbodiimide *N,N'*-dicyclohexylcarbodiimide (Fig. 23).<sup>165</sup> The bioactive CRGDS was conjugated with PEG-norbornene with a photoinitiator (Irgacure 2959) under 365 nm UV light for 3 min at  $4.5 \text{ mW cm}^{-2}$ . Subsequently, the CRGDS-conjugated PEG-norbornene, PEG-norbornene, MMP (matrix metalloproteinase)-degradable peptide (KCGGPQGIWGQGCK), and PEG-dithiol (HS-PEG-SH) crosslinker were polymerized to generate CRGDS and MMP-conjugated PEG hydrogels.<sup>165</sup> The proliferation and capillary network formation of HUVECs cultured on several types of CRGDS and MMP-conjugated PEG hydrogels were then investigated.

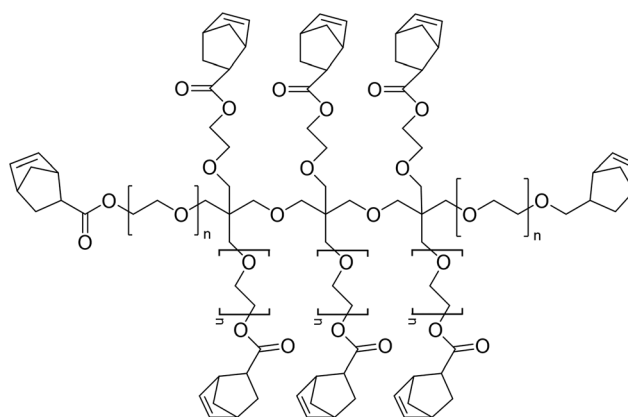


Fig. 23 Chemical scheme of 8-arm PEG-OH conjugated with norbornene.

Silva prepared GRGDS-conjugated gellan gum hydrogels<sup>216</sup> where the glucuronic acid monosaccharide of gellan gum hydrogels is activated with 4-(4,6-dimethoxy-1,3,5-triazin-2-yl)-4-methylmorpholinium chloride (DMT-MM), and subsequently, furfurylamine was conjugated on the gellan gum hydrogels. Then, the furan-gellan gum hydrogels were reacted with maleimide-conjugated GRGDS peptide to generate GRGDS-gellan gum hydrogels using Diels–Alder chemistry, where a maleimide-conjugated GRGDS peptide was synthesized from the reaction with GRGDS, maleimidopropionic acid and diisopropylcarbodiimide.<sup>216</sup> GRGDS-gellan gum hydrogels supported the proliferation of rat NPSCs.<sup>216</sup> The introduction of a joint segment (GG or GGGG) between the bioactive GRGDS and gellan gum hydrogel might significantly improve the NPSC attachment, proliferation and differentiation observed in the study.

Tam *et al.* prepared hyaluronan-methyl cellulose hydrogels conjugated with bioactive peptides and growth factors where methyl cellulose was chemically converted to carboxylated-methyl cellulose.<sup>221</sup> Then, sulfhydryl-methylcellulose was prepared from the carboxylated-methyl cellulose using 4-(4,6-dimethoxy-1,3,5-triazin-2-yl)-4-methylmorpholinium chloride (DMT-MM), 3,3'-dithiobis(propionic acid dihydrazide), and dithiothreitol. Subsequently, maleimide-streptavidin and maleimide-GRGDS were added to sulfhydryl-methylcellulose to generate GRGDS- and streptavidin-conjugated methylcellulose using the thiol-maleimide click reaction (Fig. 19).<sup>221</sup> Furthermore, recombinant platelet-derived growth factor A (rPDGF-A) was conjugated into GRGDS- and streptavidin-conjugated methylcellulose after rPDGF-A was conjugated with biotin. Finally, GRGDS- and rPDGF-A-conjugated methyl cellulose and hyaluronan were blended for their experiments.<sup>221</sup> Improved differentiation of rat NPSCs into oligodendrocytes was observed in hydrogels conjugated with GRGDS and rPDGF-A compared to the hydrogels without conjugation of GRGDS and rPDGF-A.

Li *et al.* prepared PEG hydrogels conjugated with a short laminin peptide (CCRRIKVAVWLC), where four-arm thiolated PEG was crosslinked by PEG tetraacrylate and partially conjugated with the peptide.<sup>1</sup> The acrylate in PEG tetraacrylate conjugated with the thiol group of four-arm thiolated PEG and the peptide from the thiol-ene reaction (Michael-type addition reaction). Human NSPCs could attach and proliferate on PEG hydrogels conjugated with the short laminin peptide and efficiently differentiated into neurons on the hydrogels.<sup>1</sup>

Zhang prepared injectable hydroxyethylmethacrylate (HEMA)-*g*-poly(L-lactic acid) (HEMA-PLLA) nanofibrous hollow microspheres<sup>257</sup> where growth factor mimicking peptides (TGF- $\beta$ 1-mimicking peptide (Cytomodulin-10, LIANAK) and bone morphogenic protein-2 (BMP-2) mimicking peptide (P24, KIPKASSVPTLSAISTLYLSSGGC)) are grafted using the click reaction (thiol-ene reaction) (Fig. 19) of thiol from cysteine-bioactive peptide conjugate and alkene from acrylate grafting on HEMA-PLLA nanofibrous microspheres. The acrylic HEMA-PLLA nanofibrous microspheres were prepared by the reaction of methacrylic anhydride with hydroxy groups of HEMA-PLLA nanofibrous microspheres.<sup>257</sup> Hyaline cartilage was effectively formed in nude mice by subcutaneous

implantation of rabbit BMSCs with cytomodulin-10-grafted HEMA-PLLA nanofibrous hollow microspheres, whereas bone regeneration was clearly observed in nude mice by subcutaneous implantation of rabbit BMSCs with P24-grafted HEMA-PLLA nanofibrous hollow microspheres.<sup>257</sup> The growth factor-mimicking peptides, which were grafted with optimal nanofibrous hollow microspheres, work effectively to direct stem cell differentiation for specific tissue regeneration.

HyA is one of the components of the ECM, and HyA hydrogels have anti-inflammatory effects and inhibitory effects on glial scar formation in the central nervous system. Although HyA can bind the cell receptor CD44, the binding ability of HyA to the cells is not sufficient. Therefore, Li *et al.* introduced the laminin-5  $\alpha$ 3 chain-derived peptide PPFLMLLKGSTR onto HyA hydrogels,<sup>104</sup> of which the main binding site is  $\alpha$ 3 $\beta$ 1 integrin of the cells; the HyA hydrogels were prepared by crosslinking HyA using adipic dihydrazide. Subsequently, the bioactive peptide PPFLMLLKGSTR was conjugated to crosslinked HyA hydrogels with 1,10-carbonyldiimidazole. Rat BMSCs in the HyA hydrogel scaffolds conjugated with PPFLMLLKGSTR showed better survival and adhesion than the cells in nonmodified HyA hydrogels did.<sup>104</sup> Rat BMSCs in HyA hydrogel scaffolds conjugated with PPFLMLLKGSTR were implanted in the transected spinal cord of Sprague Dawley (SD) rats. The transplanted cells were restored in injured spinal cord tissue, and hindlimb motor function was significantly improved with the use of HyA hydrogel scaffolds conjugated with PPFLMLLKGSTR compared to the use of nonmodified HyA hydrogel scaffolds.<sup>104</sup> A comparison of the results using other peptide-conjugated HyA hydrogel scaffolds such as HyA hydrogel scaffolds conjugated with RGDSP, IKVAV, YIGSR with and without a joining segment (GG or GGGG) would clarify the advantage of HyA hydrogels conjugated with PPFLMLLKGSTR for the treatment of spinal cord injuries in SD rats.

#### 4.2. Stem cells on the material surface grafted with peptides

In several studies,<sup>68,94,161</sup> multiple peptide sequences have been developed from ECM proteins and grafted onto polymeric films, glass, implants, scaffolds and nanofibers. hPSCs were then directly cultured on the peptide-grafted surfaces for several passages, allowing the effective bioactive peptides to be identified.

Chung *et al.* grafted a cell-adhesive peptide GRGD on a blend film of polyurethane (PU) and PEG.<sup>213</sup> The GRGD peptide was activated with the reaction of *N*-succinimidyl-6-[4'-azido-2'-nitrophenylamino]-hexanoate (SANPAH) (Fig. 14 and 20), which introduces an azide group on the peptide. The SANPAH-GRGD solution was adsorbed on the PU-PEG blend film surface, and subsequently, the PU-PEG blend film surface was irradiated with UV light for photoreaction.<sup>213</sup> HUVECs showed better adhesion to the GRGD-grafted PU-PEG blend film surface than to the film without GRGD grafting.

Melkounian *et al.* developed polyacrylate surfaces grafted with several bioactive peptides using EDC/NHS chemistry, where these peptides were derived from bone sialoprotein (KGGNGEPRGDTYRAY (BSP-1) and PEO4-NGEPRGDTYRAY (BSP-2)), vitronectin (KGGPQVTRGDVFTMP (VN-1)), fibronectin

(GRGDSPK (FN-1) and KGGAVTGRGDSPASS (FN-2)) and laminin (KYGAASIKVAVSADR (LN-1)), which were taken from the literature.<sup>94</sup> The peptides BSP-1, BSP-2, VN-1, FN-1 and FN-2 contain the RGD motif, whereas the peptide LN-1 contains the laminin motif IKVAV. BSP-2 has a joint segment of PEO4.

hESC attachment to the polyacrylate surface grafted with BSP-1, BSP-2 and VN-1 was found to be similar to attachment to Matrigel-coated dishes, whereas poor hESC attachment was found on the polyacrylated surface grafted with FN-1, FN-2 and LN-1.<sup>94</sup> It should be noted that a high concentration peptide solution is necessary to prepare the grafted polyacrylated surface, such as more than 0.5 mM, which corresponds to 1000  $\mu\text{g mL}^{-1}$  and 1200  $\mu\text{g mL}^{-1}$  for BSP-1 and VN-1 solutions, respectively. The concentrations of recombinant vitronectin or laminin-521 solution for coating ECMs are more than two orders of magnitude less, such as 5 or 20  $\mu\text{g mL}^{-1}$ .

hESCs could be cultivated on the polyacrylate surface grafted with BSP-1 and VN-1 in chemically defined medium for over 12 passages with a doubling time of approximately 40 h and a maintained pluripotency, which are results similar to those of hESCs cultured on Matrigel-coated dishes (the gold standard for hPSC culture).<sup>94</sup>

Although hESCs could not attach to and proliferate on the polyacrylate surface grafted with laminin-derived peptide, better selection of the bioactive peptides derived from laminin, such as those containing the RGD motif, will support hPSC adhesion and proliferation, as reported previously.<sup>68,87,88</sup>

Peptides can be covalently conjugated on clean glass. In one study, after treating a glass plate with trifluoroacetic acid, the surface was treated with (3-aminopropyl)triethoxysilane to generate an amino segment-grafted surface. Subsequently, the bioactive peptide can be conjugated with amino groups using the reagents 2-(1*H*-benzotriazol-1-yl)-1,1,3,3-tetramethyluronium hexafluorophosphate (HBTU), 1-hydroxybenzotriazole (HOBt), and *N,N*-diisopropylethylamine (DIPEA).<sup>284</sup> Zamuner *et al.* prepared glass plates, which were covalently conjugated with a proteolytically stable osteoblast-adhesive peptide, YGKRNTHR-FYGKRNTHRF, using this surface reaction method.<sup>284</sup>

Okano *et al.* prepared a temperature-responsive cell culture surface containing the cell binding site RGDS,<sup>285</sup> which enabled controlled detachment of the cells by reducing the temperature below the lower solution critical temperature (LCST) of the thermoresponsive segments grafted on the surface. In this case, *N*-isopropylacrylamide and 2-carboxyisopropylacrylamide were grafted onto the TCPS surface using electron beam irradiation. Subsequently, RGDS was bonded to the carboxylic acid of 2-carboxyisopropylacrylamide using a water soluble carbodiimide (1-ethyl-3-(3-dimethylaminopropyl)carbodiimide). When HUVECs were cultured on a poly(*N*-isopropylacrylamide-co-2-carboxyisopropylacrylamide) surface conjugated with RGDS, HUVECs could be successively detached from the thermoresponsive surface at a lower temperature (20 degrees), where poly-*N*-isopropylacrylamide contributed to the thermoresponsive site on the cell culture surface.

Becker *et al.* grafted bioactive peptides onto polyether ketone (PEEK) disks.<sup>210</sup> Because PEEK contains a ketone group

(Fig. 8), ethylene diamine was conjugated on the PEEK surface using a Schiff base reaction.<sup>286–288</sup> Subsequently, diethylene glycol diglycidyl ether (DGDE) (Fig. 14) was reacted with the amino group on PEEK, where the head group of epoxy was reacted with the amino group of the peptide (RGD). In this reaction, the compound 3-(2-pyridyldithio)propionamido-PEG4-NHS ester *N*-succinimidyl 3-oxo-1-(pyridin-2-ylidysulfanyl)-7,10,13,16-tetraoxa-4-azanodecan-19-oate 3-oxo-1-(pyridin-2-ylidysulfanyl)-7,10,13,16-tetraoxa-4-azanodecan-19-oic acid *N*-succinimidyl ester (PEG4-SPDP) (Fig. 14) might be used instead of DGDE, and SGRGD is conjugated on the PEEK surface. In this case, a joint segment of (PEG)<sub>4</sub> may effectively support the binding of the cells and SGRGD.

Several researchers have used a mussel-inspired immobilization method on material surfaces.<sup>201,289,290</sup> Poly-3,4-dihydroxy-*L*-phenylalanine (*L*-pDOPA) is a main component of mussel adhesive materials. 3,4-Dihydroxy-*L*-phenylalanine (*L*-DOPA) can be polymerized in alkaline conditions, such as at the pH of marine environments, by oxidative conversion of catecholamines to quinones. *L*-pDOPA can be coated onto biomaterial surfaces in a thin layer. Furthermore, amine, thiol and imidazole groups can be covalently bonded to catechol groups on an *L*-pDOPA layer. Therefore, Ko *et al.* prepared a PLGA scaffold where *L*-pDOPA was coated on PLGA scaffolds by immersing of the scaffolds into *L*-DOPA and the subsequent spontaneous polymerization of *L*-DOPA.<sup>201</sup> Subsequently, *L*-pDOPA-coated PLGA scaffolds were immersed in BMP-2 peptide solution, and BMP-2 peptide was conjugated to *L*-pDOPA-coated PLGA (BMP-2-pDOPA-PLGA) scaffolds by Michael-type addition. hADSCs in BMP-2-pDOPA-PLGA scaffolds showed improved *in vitro* osteogenic differentiation and *in vivo* bone formation in critical-sized calvarial bone defects.<sup>201</sup>

Barati *et al.* prepared poly(DL-lactide)-conjugated EEGGC,<sup>130</sup> which is the nucleating peptide of calcium phosphate, and electrospun poly(DL-lactide) (PLA)-conjugated EEGGC to generate nanofibers for calcium phosphate nucleation and osteogenic differentiation of hBMSCs, where PLA was reacted with acryloyl chloride to generate acrylate-terminated PLA. Subsequently, the EEGGC peptide was conjugated with acrylate-terminated PLA by a Michael addition reaction.

Another method to immobilize peptides on a material surface is to use the avidin–biotin reaction. Wrighton *et al.* prepared streptavidin-coated PS dishes<sup>291</sup> where streptavidin is a 53 kDa protein; therefore, the coated dishes can be prepared by just insertion (coating) of the streptavidin solution into PS dishes. Then, the biotinylated linker solution, such as biotinyl-6-aminohexanoic acid and biotinyl-8-amino-3,6-dioxaoctanoic acid, was injected into the streptavidin-coated PS dishes. Because the head site of the biotinylated linker is a carboxylic acid and will be immobilized on streptavidin-coated PS dishes, the amino group of peptides can be conjugated with the cap carboxylic acid on the biotinylated linker. This reaction for the preparation of peptide-immobilized PS dishes can be done in an aqueous solution.

There are several other methods to graft bioactive peptides onto materials. Kim *et al.* polymerized glycidyl methacrylate on

a surface (in this case, polyurethane acrylate).<sup>292</sup> Subsequently, the osteoinductive peptide BMP-2 was added to the polyglycidyl methacrylate (PGM). BMP-2 was conjugated to the PGM surface by the reaction of the epoxy group in PGM and the amine group of BMP-2.

Klim *et al.* prepared several SAM surfaces consisting of alkanethiol-conjugated peptides to investigate optimal bioactive peptide sequences<sup>225</sup> that supported the adhesion and proliferation of hPSCs. They prepared SAMs using 18 different bioactive peptides, which were derived from NCAM (NCAM-1, GGGEVYVVAENQQKSKA), bone morphogenetic-2 (BMP-1, KIPKASSVPTLSAISTLYL), Dkk-1 (Dkk-1, LSSKMYHTKGQEGSVLSRSSD), phage display (PD-1, ADSQLIHGGLRS; PD-2, MHRMPSFLPTTL), *N*-cadherin (CAD-1, INPISGQ), occludin (OC-1, GSQIYALCNQFYTPAATGLYVD), E-cadherin (CAD-2, ATYTLFSHAVSSNGNAV), annexin (ANX-1, GGSTVHEILSKLSLEG), combinatorial chemistry (CC-1, GGGKHIFSDDSSE), fibronectin (FN-3, KPHSRN; FN-4, GWQPPRARI; FN-5, GGPEILDVPST), vitronectin (HBP-1, GKKQRFRRHRNRKG), laminin (LN-2, GSDPGYIGSR; LN-3, GGIKVAV), BSP (BSP-3, FHRRIKA), and fibronectin/vitronectin (FVN-1, KGRGDS). Among the 18 peptides, only FVN-1 contained RGD.

The SAM surfaces prepared from heparin-binding peptides (HBP-1, BSP-3 and FN-4) could extensively support hESC attachment and proliferation, maintaining pluripotency in mTeSR1 media containing Y-27632 (ROCK inhibitor), whereas the SAM surface prepared with the integrin ligand KGRGDS (FVN-1) could not maintain the pluripotency of hESCs.<sup>225</sup> Several hESC lines (DF19-97T, H14, H13, H9) and hiPSCs (IMR-90) were cultured on plates immobilized with the HBP-1 peptide using streptavidin-biotin chemistry in mTeSR1 together with Y-27632. Extensive proliferation of hPSCs was found over 3 months (17 passages), and their pluripotency and normal karyotypes were maintained.<sup>225</sup> These cells could differentiate into cells derived from three germ layer lineages after 3 months of culture. The hESCs could also be cultured on the surface immobilized with HBP-1 peptide and the cyclic RGD peptide for two months in mTeSR1 medium without a ROCK inhibitor; and the hESCs maintained their self-renewal characteristics while maintaining pluripotency and normal karyotypes.<sup>225</sup> Specific peptide-immobilized plates, which do not contain RGD moieties, can also support hPSC proliferation and pluripotency in a chemically defined medium and are preferable compared to ECM-immobilized plates because of their fully synthetic properties.

## 5. Conclusions

The development of synthetic ECM protein-derived peptides that mimic the biological and biochemical functions of natural ECM proteins is important for academic interest and future clinical application. Peptides derived from or inspired by specific ECM proteins act as agonists of each ECM protein receptor. Given that most ECM proteins function in cell adhesion *via* integrin receptors, many peptides have been developed that bind to specific integrin receptors. We discussed the

peptide sequence, immobilization design, reaction method, and functions of several ECM protein-derived peptides. Not only specific sequences of ECM-derived peptides but also joint segments and immobilization methods, including specific grafting reactions, are important. Typically, the 4G sequence is optimal as a joint segment for the grafting of bioactive peptides onto biomaterials or biomacromolecules. The carbodiimide reaction using EDC/NHS and EDC/sulfo-NHS is the most popular reaction for the grafting of bioactive ECM-derived peptides on material surfaces. This is because ECM-derived peptides have an amino group on one end and a carboxylic acid group on the other, which can react with EDC and NHS (or sulfo-NHS). This reaction can be performed under very mild conditions, such as in aqueous solutions at ambient temperature, with no requirement for heavy metal catalysts. The next most popular reaction is the thiol-ene reaction, including the maleimide-thiol reaction, which is called Michael-type addition or a click reaction. Typically, cysteine is added to bioactive ECM-derived peptides, and maleimide or other functional groups containing double bonds are grafted onto the material surface. Then, the ECM-derived peptides spontaneously react with double bonds on the material, causing the immobilization of ECM-derived peptides on the material.

In most cases, ECM proteins with high molecular weights can be immobilized on a material surface using a very low concentration ECM protein solution, such as 5–20  $\mu\text{g mL}^{-1}$ , whereas smaller ECM-derived peptides need to be in a solution with a concentration 1–2 orders of magnitude higher for immobilization on a material surface using both the coating method and grafting method. This is likely due to the difference in the binding affinity of stem cells for ECM proteins and ECM-derived peptides. ECM-derived peptides cannot bind to specific integrin receptors because their conformation is too flexible, unlike ECM proteins. However, the improved design of peptide grafting on the surface might reduce the grafting or coating concentration of ECM-derived peptides in the future, which is a topic for future study in the field of peptide design and immobilization (grafting) methods.

ECM-derived peptide-immobilized materials, such as not only 2D culture dishes but also scaffolds, hydrogels, implants and nanofibers, will be used in stem cell culture and differentiation for academic purposes and clinical applications. There will likely be a high clinical demand for improved cell adhesion to implants and scaffolds by ECM protein-derived peptide immobilization. Furthermore, the materials immobilized with ECM protein-derived peptides will be useful for the efficient differentiation of hPSCs into cells with relatively lower adhesion, such as neural cells, cardiomyocytes and  $\beta$  cells, since the cell adhesion of the differentiated cells can be increased.

## Author contributions

Conceptualization: A. H. Funding acquisition: A. H., S. H. Investigation: T. S., T. W., Q. L., S. K. S., R. R. R. Supervision:



Q. L., A.U., S.H. Writing—original draft: T. S., T. W., Q. L., A. H. Writing—review & editing: A. H.

## Conflicts of interest

There are no conflicts to declare.

## Acknowledgements

This work was supported by the Taiwan Landseed Hospital Project (NCU-LSH-111-B-00), Tri-Service General Hospital Project (111-NCU-TRI-01), and Veterans General Hospitals and University System of Taiwan Joint Research Program (VGHUST111-G4-2-1). This study was also supported by the Project of State Key Laboratory of Ophthalmology, Optometry and Vision Science, Wenzhou Medical University (No. J02-20210201) and the Wenzhou Municipal Science and Technology Bureau (Y2020227, Y2020920).

## Notes and references

- X. W. Li, X. Y. Liu, B. Josey, C. J. Chou, Y. Tan, N. Zhang and X. J. Wen, *Stem Cells Transl. Med.*, 2014, **3**, 662–670.
- A. Higuchi, Q. D. Ling, Y. Chang, S. T. Hsu and A. Umezawa, *Chem. Rev.*, 2013, **113**, 3297–3328.
- A. Higuchi, S. S. Kumar, G. Benelli, Q. D. Ling, H. F. Li, A. A. Alarfaj, M. A. Munusamy, T. C. Sung, Y. Chang and K. Murugan, *Prog. Mater. Sci.*, 2019, **103**, 374–424.
- A. Higuchi, S. S. Kumar, Q. D. Ling, A. A. Alarfaj, M. A. Munusamy, K. Murugan, S. T. Hsu, G. Benelli and A. Umezawa, *Prog. Polym. Sci.*, 2017, **65**, 83–126.
- M. A. Skylar-Scott, J. Y. Huang, A. Lu, A. H. M. Ng, T. Duenki, S. Liu, L. L. Nam, S. Damaraju, G. M. Church and J. A. Lewis, *Nat. Biomed. Eng.*, 2022, **6**, 449–462.
- J. Lee, W. H. van der Valk, S. A. Serdy, C. Deakin, J. Kim, A. P. Le and K. R. Koehler, *Nat. Protoc.*, 2022, **17**, 1266–1305.
- B. Bohl, A. Jabali, J. Ladewig and P. Koch, *Sci. Adv.*, 2022, **8**, eabl5792.
- Q. Wu, Y. Shichino, T. Abe, T. Suetsugu, A. Omori, H. Kiyonari, S. Iwasaki and F. Matsuzaki, *Nat. Commun.*, 2022, **13**, 470.
- S. Song, K. W. McConnell, D. Amores, A. Levinson, H. Vogel, M. Quarta, T. A. Rando and P. M. George, *Biomaterials*, 2021, **275**, 120982.
- Y. T. Wang, T. Yoshitomi, N. Kawazoe, Y. N. Yang and G. P. Chen, *Adv. Mater. Interfaces*, 2022, **9**, 2101978.
- Y. Chen, K. Lee, N. Kawazoe, Y. Yang and G. Chen, *J. Mater. Chem. B*, 2019, **7**, 7195–7206.
- Y. Xu, J. Dai, X. S. Zhu, R. F. Cao, N. Song, M. Liu, X. G. Liu, J. J. Zhu, F. Pan, L. L. Qin, G. N. Jiang, H. F. Wang and Y. Yang, *Adv. Mater.*, 2022, **34**, e2106755.
- S. Kim, S. Lee, J. Lim, H. Choi, H. Kang, N. Li Jeon and Y. Son, *Biomaterials*, 2021, **279**, 121210.
- Y. Wu, L. Xie, M. Wang, Q. Xiong, Y. Guo, Y. Liang, J. Li, R. Sheng, P. Deng, Y. Wang, R. Zheng, Y. Jiang, L. Ye, Q. Chen, X. Zhou, S. Lin and Q. Yuan, *Nat. Commun.*, 2018, **9**, 4772.
- A. Y. Clark, K. E. Martin, J. R. Garcia, C. T. Johnson, H. S. Theriault, W. M. Han, D. W. Zhou, E. A. Botchwey and A. J. Garcia, *Nat. Commun.*, 2020, **11**, 114.
- J. Xing, Y. Ying, C. Mao, Y. Liu, T. Wang, Q. Zhao, X. Zhang, F. Yan and H. Zhang, *Nat. Commun.*, 2018, **9**, 2020.
- J. Pan, Y. C. Lee, H. H. Lee, T. C. Sung, S. H. Jen, L. K. Ban, H. Y. Su, D. C. Chen, S. T. Hsu, A. Higuchi and H. Chen, *J. Mater. Chem. B*, 2020, **8**, 5204–5214.
- Y. Gao, N. J. Ku, T. C. Sung, A. Higuchi, C. S. Hung, H. H. Lee, Q. D. Ling, N. C. Cheng, A. Umezawa, L. Barro, T. Burnouf, Q. Ye and H. Chen, *J. Mater. Chem. B*, 2019, **7**, 7110–7119.
- J. Lee, S. Lee, T. Ahmad, S. K. Madhurakkat Perikamana, J. Lee, E. M. Kim and H. Shin, *Biomaterials*, 2020, **255**, 120192.
- S. J. Kim, J. Park, H. Byun, Y. W. Park, L. G. Major, D. Y. Lee, Y. S. Choi and H. Shin, *Biomaterials*, 2019, **188**, 198–212.
- M. Zolfaghar, L. Mirzaeian, B. Beiki, T. Najji, A. Moini, P. Eftekhari-Yazdi, V. Akbarinejad, A. J. Vernengo and R. Fathi, *Heliyon*, 2020, **6**, e04992.
- D. W. Kim, M. Staples, K. Shinozuka, P. Pantcheva, S. D. Kang and C. V. Borlongan, *Inter. J. Molecular Sci.*, 2013, **14**, 11692–11712.
- K. Stefanska, K. Ozegowska, G. Hutchings, M. Popis, L. Moncrieff, C. Dompe, K. Janowicz, W. Pienkowski, P. Gutaj, J. A. Shibli, W. M. Prado, H. Piotrowska-Kempisty, P. Mozdziak, M. Bruska, M. Zabel, B. Kempisty and M. Nowicki, *J. Clin. Med.*, 2020, **9**, 1102.
- M. M. Kamal and D. H. Kassem, *Front. Cell Dev. Biol.*, 2020, **8**, 16.
- S. Muduli, H. H. C. Lee, J. S. Yang, T. Y. Chen, A. Higuchi, S. S. Kumar, A. A. Alarfaj, M. A. Munusamy, G. Benelli, K. Murugan, C. Y. Liu, Y. F. Chen, Y. Chang, B. Moorthy, H. C. Wang, S. T. Hsu and Q. D. Ling, *J. Mater. Chem. B*, 2017, **5**, 5345–5354.
- Y. Xu, J. Xiang, H. Zhao, H. Liang, J. Huang, Y. Li, J. Pan, H. Zhou, X. Zhang, J. H. Wang, Z. Liu and J. Wang, *Biomaterials*, 2016, **100**, 91–100.
- M. Zavatti, F. Beretti, F. Casciaro, E. Bertucci and T. Maraldi, *BioFactors*, 2020, **46**, 106–117.
- C. Balbi, K. Lodder, A. Costa, S. Moimas, F. Moccia, T. van Herwaarden, V. Rosti, F. Campagnoli, A. Palmeri, P. De Biasio, F. Santini, M. Giacca, M. J. Goumans, L. Barile, A. M. Smits and S. Bollini, *Inter. J. Cardiology*, 2019, **287**, 87–95.
- W. C. Shen, Y. C. Lai, L. H. Li, K. Liao, H. C. Lai, S. Y. Kao, J. Wang, C. M. Chuong and S. C. Hung, *Nat. Commun.*, 2019, **10**, 2226.
- X. Lan, Z. Sun, C. Chu, J. Boltze and S. Li, *Front. Neurol.*, 2019, **10**, 824.
- H. Guo, B. Li, M. Wu, W. Zhao, X. He, B. Sui, Z. Dong, L. Wang, S. Shi, X. Huang, X. Liu, Z. Li, X. Guo, K. Xuan and Y. Jin, *Biomaterials*, 2021, **279**, 121223.

- 32 R. Zhang, L. Xie, H. Wu, T. Yang, Q. Zhang, Y. Tian, Y. Liu, X. Han, W. Guo, M. He, S. Liu and W. Tian, *Acta Biomater.*, 2020, **113**, 305–316.
- 33 N. T. Awatade, S. L. Wong, C. K. Hewson, L. K. Fawcett, A. Kicic, A. Jaffe and S. A. Waters, *Front. Pharmacol.*, 2018, **9**, 1429.
- 34 L. C. Rijsbergen, L. L. A. van Dijk, M. F. M. Engel, R. D. de Vries and R. L. de Swart, *Front. Immunol.*, 2021, **12**, 683002.
- 35 J. A. Mitchel, A. Das, M. J. O'Sullivan, I. T. Stancil, S. J. DeCamp, S. Koehler, O. H. Ocana, J. P. Butler, J. J. Fredberg, M. A. Nieto, D. P. Bi and J. A. Park, *Nat. Commun.*, 2020, **11**, 5053.
- 36 J. M. Kress, L. D. Dio, L. Heck, A. Pulliero, A. Izzotti, K. Laarmann, G. Fritz and B. Kaina, *Sci. Rep.*, 2019, **9**, 13800.
- 37 W. Sievert, S. Tapio, S. Breuninger, U. Gaipl, N. Andratschke, K. R. Trott and G. Multhoff, *PLoS One*, 2014, **9**, e91808.
- 38 N. Goshi, R. K. Morgan, P. J. Lein and E. Seker, *J. Neuroinflammation*, 2020, **17**, 155.
- 39 E. Moutin, A. L. Hemonnot, V. Seube, N. Linck, F. Rassendren, J. Perroy and V. Compan, *Front. Synaptic Neurosci.*, 2020, **12**, 19.
- 40 M. P. Sahu, O. Nikkila, S. Lagas, S. Kolehmainen and E. Castren, *Neuronal Signaling*, 2019, **3**, NS20180207.
- 41 D. L. McPhie, R. Nehme, C. Ravichandran, S. M. Babb, S. D. Ghosh, A. Staskus, A. Kalinowski, R. Kaur, P. Douvaras, F. Du, D. Ongur, V. Fossati, K. Eggan and B. M. Cohen, *Transl. Psychiatry*, 2018, **8**, 230.
- 42 Y. Zhang, X. Y. Lu, G. Casella, J. Tian, Z. Q. Ye, T. Yang, J. J. Han, L. Y. Jia, A. Rostami and X. Li, *Front. Cell. Neurosci.*, 2019, **13**, 247.
- 43 X. Chamling, A. Kallman, W. Fang, C. A. Berlinicke, J. L. Mertz, P. Devkota, I. E. M. Pantoja, M. D. Smith, Z. Ji, C. Chang, A. Kaushik, L. Chen, K. A. Whartenby, P. A. Calabresi, H. Q. Mao, H. Ji, T. H. Wang and D. J. Zack, *Nat. Commun.*, 2021, **12**, 652.
- 44 J. A. Garcia-Leon, B. Garcia-Diaz, K. Eggermont, L. Caceres-Palomo, K. Neyrinck, R. Madeiro da Costa, J. C. Davila, A. Baron-Van Evercooren, A. Gutierrez and C. M. Verfaillie, *Nat. Protoc.*, 2020, **15**, 3716–3744.
- 45 E. N. Smith, A. D'Antonio-Chronowska, W. W. Greenwald, V. Borja, L. R. Aguiar, R. Pogue, H. Matsui, P. Benaglio, S. Borooh, M. D'Antonio, R. Ayyagari and K. A. Frazer, *Stem Cell Rep.*, 2019, **12**, 1342–1353.
- 46 F. Michelet, A. Balasankar, N. Teo, L. W. Stanton and S. Singhal, *Stem Cell Res. Ther.*, 2020, **11**, 47.
- 47 L. da Cruz, K. Fynes, O. Georgiadis, J. Kerby, Y. H. Luo, A. Ahmado, A. Vernon, J. T. Daniels, B. Nommiste, S. M. Hasan, S. B. Gooljar, A. F. Carr, A. Vugler, C. M. Ramsden, M. Bictash, M. Fenster, J. Steer, T. Harbinson, A. Wilbrey, A. Tufail, G. Feng, M. Whitlock, A. G. Robson, G. E. Holder, M. S. Sagoo, P. T. Loudon, P. Whiting and P. J. Coffey, *Nat. Biotechnol.*, 2018, **36**, 328–337.
- 48 D. Balboa, D. G. Iworima and T. J. Kieffer, *Front. Endocrinol.*, 2021, **12**, 642152.
- 49 D. Balboa, T. Barsby, V. Lithovius, J. Saarimaki-Vire, M. Omar-Hmeadi, O. Dyachok, H. Montaser, P. E. Lund, M. Yang, H. Ibrahim, A. Naatanen, V. Chandra, H. Vihinen, E. Jokitalo, J. Kvist, J. Ustinov, A. I. Nieminen, E. Kuuluvainen, V. Hietakangas, P. Katajisto, J. Lau, P. O. Carlsson, S. Barg, A. Tengholm and T. Otonkoski, *Nat. Biotechnol.*, 2022, **40**, 1042–1055.
- 50 Y. Du, Z. Liang, S. Wang, D. Sun, X. Wang, S. Y. Liew, S. Lu, S. Wu, Y. Jiang, Y. Wang, B. Zhang, W. Yu, Z. Lu, Y. Pu, Y. Zhang, H. Long, S. Xiao, R. Liang, Z. Zhang, J. Guan, J. Wang, H. Ren, Y. Wei, J. Zhao, S. Sun, T. Liu, G. Meng, L. Wang, J. Gu, T. Wang, Y. Liu, C. Li, C. Tang, Z. Shen, X. Peng and H. Deng, *Nat. Med.*, 2022, **28**, 272–282.
- 51 Q. N. J. Hogrebe, K. G. Maxwell, P. Augsornworawat and J. R. Millman, *Nat. Protoc.*, 2021, **16**, 4109–4143.
- 52 E. A. Rosado-Olivieri, K. Anderson, J. H. Kenty and D. A. Melton, *Nat. Commun.*, 2019, **10**, 1464.
- 53 T. Brecklinghaus, W. Albrecht, F. Kappenberg, J. Duda, M. Zhang, I. Gardner, R. Marchan, A. Ghallab, O. Demirci Turgunbayer, J. Rahnenfuhrer and J. G. Hengstler, *Toxicol. In Vitro*, 2022, **81**, 105344.
- 54 S. Su, C. Di Poto, R. Roy, X. F. Liu, W. X. Cui, A. Kroemer and H. W. Ransom, *Exp. Biol. Med.*, 2019, **244**, 857–864.
- 55 M. Klaas, K. Moll, K. Maemets-Allas, M. Loog, M. Jarvekulg and V. Jaks, *Sci. Rep.*, 2021, **11**, 20165.
- 56 Y. Li, Q. Wu, Y. Wang, H. Bu and J. Bao, *Methods Mol. Biol.*, 2020, **2110**, 267–287.
- 57 G. F. Wei, J. W. Wang, Q. Lv, M. Liu, H. Xu, H. Zhang, L. L. Jin, J. C. Yu and X. L. Wang, *J. Biomed. Mater. Res., Part A*, 2018, **106**, 2171–2180.
- 58 J. Cooper and F. G. Giancotti, *Cancer Cell*, 2019, **35**, 347–367.
- 59 F. Martino, A. R. Perestrelo, V. Vinarsky, S. Pagliari and G. Forte, *Front. Physiol.*, 2018, **9**, 824.
- 60 A. Ramasubramanian, R. Muckom, C. Sugnaux, C. Fuentes, B. L. Ekerdt, D. S. Clark, K. E. Healy and D. V. Schaffer, *ACS Biomater. Sci. Eng.*, 2021, **7**, 1344–1360.
- 61 L. Hagbard, K. Cameron, P. August, C. Penton, M. Parmar, D. C. Hay and T. Kallur, *Philos. Trans. R. Soc., B*, 2018, **373**, 20170230.
- 62 A. Srinivasan and Y. C. Toh, *Front. Mol. Neurosci.*, 2019, **12**, 39.
- 63 T. Hyvarinen, A. Hyysalo, F. E. Kapucu, L. Aarnos, A. Vinogradov, S. J. Eglén, L. Yla-Outinen and S. Narkilahti, *Sci. Rep.*, 2019, **9**, 17125.
- 64 T. C. Sung, C. H. Liu, W. L. Huang, Y. C. Lee, S. S. Kumar, Y. Chang, Q. D. Ling, S. T. Hsu and A. Higuchi, *Biomater. Sci.*, 2019, **7**, 5467–5481.
- 65 S. Bhattacharya, P. W. Burrridge, E. M. Kropp, S. L. Chuppa, W. M. Kwok, J. C. Wu, K. R. Boheler and R. L. Gundry, *J. Vis. Exp.*, 2014, **91**, 52010.
- 66 T. C. Sung, H. C. Su, Q. D. Ling, S. S. Kumar, Y. Chang, S. T. Hsu and A. Higuchi, *Biomaterials*, 2020, **253**, 120060.
- 67 P. W. Burrridge, E. Matsa, P. Shukla, Z. C. Lin, J. M. Churko, A. D. Ebert, F. Lan, S. Diecke, B. Huber, N. M. Mordwinkin, J. R. Plews, O. J. Abilez, B. Cui, J. D. Gold and J. C. Wu, *Nat. Methods*, 2014, **11**, 855–860.

- 68 T. C. Sung, M. W. Lu, Z. Tian, H. H. Lee, J. Pan, Q. D. Ling and A. Higuchi, *J. Mater. Chem. B*, 2021, **9**, 7662–7673.
- 69 A. Higuchi, Q. D. Ling, Y. A. Ko, Y. Chang and A. Umezawa, *Chem. Rev.*, 2011, **111**, 3021–3035.
- 70 A. Higuchi, Q. D. Ling, S. Kumar, M. Munusamy, A. A. Alarfajj, A. Umezawa and G. J. Wu, *Prog. Polym. Sci.*, 2014, **39**, 1348–1374.
- 71 M. Nomizu, W. H. Kim, K. Yamamura, A. Utani, S. Y. Song, A. Otaka, P. P. Roller, H. K. Kleinman and Y. Yamada, *J. Biol. Chem.*, 1995, **270**, 20583–20590.
- 72 B. S. Weeks, J. B. Kopp, S. Horikoshi, F. B. Cannon, M. Garrett, H. K. Kleinman and P. E. Klotman, *Am. J. Physiol.*, 1991, **261**, F688–695.
- 73 P. Ekblom, P. Lonai and J. F. Talts, *Matrix Biol.*, 2003, **22**, 35–47.
- 74 S. Iriyama, M. Yasuda, S. Nishikawa, E. Takai, J. Hosoi and S. Amano, *Sci. Rep.*, 2020, **10**, 12592.
- 75 M. Iwamuro, H. Shiraha, M. Kobashi, S. Horiguchi and H. Okada, *Curr. Issues Mol. Biol.*, 2022, **44**, 1539–1551.
- 76 J. Chen, H. Zhang, J. Luo, X. Wu, X. Li, X. Zhao, D. Zhou and S. Yu, *Oncol. Lett.*, 2018, **16**, 199–210.
- 77 P. Rousselle and J. Y. Scoazec, *Semin. Cancer Biol.*, 2020, **62**, 149–165.
- 78 M. Aumailley, L. Bruckner-Tuderman, W. G. Carter, R. Deutzmann, D. Edgar, P. Ekblom, J. Engel, E. Engvall, E. Hohenester, J. C. Jones, H. K. Kleinman, M. P. Marinkovich, G. R. Martin, U. Mayer, G. Meneguzzi, J. H. Miner, K. Miyazaki, M. Patarroyo, M. Paulsson, V. Quaranta, J. R. Sanes, T. Sasaki, K. Sekiguchi, L. M. Sorokin, J. F. Talts, K. Tryggvason, J. Uitto, I. Virtanen, K. von der Mark, U. M. Wewer, Y. Yamada and P. D. Yurchenco, *Matrix Biol.*, 2005, **24**, 326–332.
- 79 L. K. Kanninen, R. Harjumaki, P. Peltoniemi, M. S. Bogacheva, T. Salmi, P. Porola, J. Niklander, T. Smutny, A. Urtti, M. L. Yliperttula and Y. R. Lou, *Biomaterials*, 2016, **103**, 86–100.
- 80 S. Rodin, L. Antonsson, C. Niaudet, O. E. Simonson, E. Salmela, E. M. Hansson, A. Domogatskaya, Z. Xiao, P. Damdimopoulou, M. Sheikhi, J. Inzunza, A. S. Nilsson, D. Baker, R. Kuiper, Y. Sun, E. Blennow, M. Nordenskjold, K. H. Grinnemo, J. Kere, C. Betsholtz, O. Hovatta and K. Tryggvason, *Nat. Commun.*, 2014, **5**, 3195.
- 81 J. H. Collier and T. Segura, *Biomaterials*, 2011, **32**, 4198–4204.
- 82 K. J. Lampe and S. C. Heilshorn, *Neurosci. Lett.*, 2012, **519**, 138–146.
- 83 J. J. Rice, M. M. Martino, L. De Laporte, F. Tortelli, P. S. Briquez and J. A. Hubbell, *Adv. Healthcare Mater.*, 2013, **2**, 57–71.
- 84 C. Wang, Y. Liu, Y. Fan and X. Li, *Regener. Biomater.*, 2017, **4**, 191–206.
- 85 J. Nicolas, S. Magli, L. Rabbachin, S. Sampaolesi, F. Nicotra and L. Russo, *Biomacromolecules*, 2020, **21**, 1968–1994.
- 86 K. Glotzbach, N. Stamm, R. Weberskirch and A. Faissner, *Front. Neurosci.*, 2020, **14**, 475.
- 87 J. Jia, E. J. Jeon, M. Li, D. J. Richards, S. Lee, Y. Jung, R. W. Barrs, R. Coyle, X. Li, J. C. Chou, M. J. Yost, S. Gerecht, S. W. Cho and Y. Mei, *Sci. Adv.*, 2020, **6**, eaaz5894.
- 88 J. Jia, R. C. Coyle, D. J. Richards, C. L. Berry, R. W. Barrs, J. Biggs, C. J. Chou, T. C. Trusk and Y. Mei, *Acta Biomater.*, 2016, **45**, 110–120.
- 89 H. Hayashi, I. Horinokita, Y. Yamada, K. Hamada, N. Takagi and M. Nomizu, *Exp. Cell Res.*, 2021, **400**, 112440.
- 90 S. K. Seidlits, J. Liang, R. D. Bierman, A. Sohrabi, J. Karam, S. M. Holley, C. Cepeda and C. M. Walthers, *J. Biomed. Mater. Res., Part A*, 2019, **107**, 704–718.
- 91 R. Derda, L. Li, B. P. Orner, R. L. Lewis, J. A. Thomson and L. L. Kiessling, *ACS Chem. Biol.*, 2007, **2**, 347–355.
- 92 P. Y. Puah, P. Y. Moh, C. S. Sipaut, P. C. Lee and S. E. How, *Polymers*, 2021, **13**, 3290.
- 93 L. Y. Santiago, R. W. Nowak, J. P. Rubin and K. G. Marra, *Biomaterials*, 2006, **27**, 2962–2969.
- 94 Z. Melkounian, J. L. Weber, D. M. Weber, A. G. Fadeev, Y. Zhou, P. Dolley-Sonneville, J. Yang, L. Qiu, C. A. Priest, C. Shogbon, A. W. Martin, J. Nelson, P. West, J. P. Beltzer, S. Pal and R. Brandenberger, *Nat. Biotech.*, 2010, **28**, 606–610.
- 95 W. Sun, T. Incitti, C. Migliaresi, A. Quattrone, S. Casarosa and A. Motta, *J. Tissue Eng. Regener. Med.*, 2017, **11**, 1532–1541.
- 96 S. S. Negah, P. Oliazadeh, A. J. Jahan-Abad, A. Eshaghabadi, F. Samini, S. Ghasemi, A. Asghari and A. Gorji, *Acta Biomater.*, 2019, **92**, 132–144.
- 97 F. Gelain, D. Bottai, A. Vescovi and S. Zhang, *PLoS One*, 2006, **1**, e119.
- 98 D. Varun, G. R. Srinivasan, Y. H. Tsai, H. J. Kim, J. Cutts, F. Petty, R. Merkle, N. Stephanopoulos, D. Dolezalova, M. Marsala and D. A. Brafman, *Acta Biomater.*, 2017, **48**, 120–130.
- 99 T. H. Perera, S. M. Howell and L. A. S. Callahan, *Biomacromolecules*, 2019, **20**, 3009–3020.
- 100 T. H. Perera, X. Lu, S. M. Howell, Y. E. Kurosu and L. A. S. Callahan, *Adv. Biosyst.*, 2020, **4**, e2000084.
- 101 S. S. Negah, Z. Khaksar, H. Aligholi, S. M. Sadeghi, S. M. M. Mousavi, H. Kazemi, A. J. Jahan-Abad and A. Gorji, *Mol. Neurobiol.*, 2017, **54**, 8050–8062.
- 102 H. Ruan, R. S. Xiao, X. H. Jiang, B. Zhao, K. Wu, Z. Z. Shao, Z. J. Zhang, H. Y. Duan and Y. L. Song, *Mol. Cell. Biochem.*, 2019, **450**, 199–207.
- 103 Y. Yu, S. S. Zhu, D. W. Wu, L. H. Li, C. R. Zhou and L. Lu, *Mater. Lett.*, 2020, **259**, 126891.
- 104 L. M. Li, M. Han, X. C. Jiang, X. Z. Yin, F. Chen, T. Y. Zhang, H. Ren, J. W. Zhang, T. J. Hou, Z. Chen, H. W. Ou-Yang, Y. Tabata, Y. Q. Shen and J. Q. Gao, *ACS Appl. Mater. Interfaces*, 2017, **9**, 3330–3342.
- 105 A. A. Dayem, J. Won, H. G. Goo, G. M. Yang, D. S. Seo, B. M. Jeon, H. Y. Choi, S. E. Park, K. Lim, S. H. Jang, S. B. Lee, S. B. Choi, K. Kim, G. H. Kan, G. B. Yeo, D. S. Kim and S. G. Cho, *Stem Cell Res.*, 2020, **43**, 101700.
- 106 S. P. Massia, S. S. Rao and J. A. Hubbell, *J. Biol. Chem.*, 1993, **268**, 8053–8059.
- 107 L. Zhang, W. R. Stauffer, E. P. Jane, P. J. Sammak and X. T. Cui, *Macromol. Biosci.*, 2010, **10**, 1456–1464.

- 108 A. Sharmin, N. Adnan, A. Haque, Y. Mashimo, M. Mie and E. Kobatake, *J. Biomed. Mater. Res. B*, 2020, **108**, 2691–2698.
- 109 N. T. Saleh, A. N. Sohi, E. Esmaeili, S. Karami, F. Soleimanifar and N. Nasoohi, *Biotechnol. Bioprocess Eng.*, 2019, **24**, 876–884.
- 110 G. H. Cui, S. J. Shao, J. J. Yang, J. R. Liu and H. D. Guo, *Mol. Neurobiol.*, 2016, **53**, 1108–1123.
- 111 K. Hozumi, M. Ishikawa, T. Hayashi, Y. Yamada, F. Katagiri, Y. Kikkawa and M. Nomizu, *J. Biol. Chem.*, 2012, **287**, 25111–25122.
- 112 Y. Kadoya, M. Nomizu, L. M. Sorokin, S. Yamashina and Y. Yamada, *Dev. Dyn.*, 1998, **212**, 394–402.
- 113 Q. Liu, Z. Jia, L. Duan, J. Xiong, D. Wang and Y. Ding, *Am. J. Transl. Res.*, 2018, **10**, 501–510.
- 114 W. R. Stauffer and X. T. Cui, *Biomaterials*, 2006, **27**, 2405–2413.
- 115 R. Mobasser, L. Tian, M. Soleimani, S. Ramakrishna and H. Naderi-Manesh, *Mater. Sci. Eng., C*, 2018, **84**, 80–89.
- 116 Q. Li, D. Xing, L. Ma and C. Gao, *Mater. Sci. Eng., C*, 2017, **73**, 562–568.
- 117 W. N. Yin, F. Y. Cao, K. Han, X. Zeng, R. X. Zhuo and X. Z. Zhang, *J. Mater. Chem. B*, 2014, **2**, 8434–8440.
- 118 M. E. Hasenbein, T. T. Andersen and R. Bizios, *Biomaterials*, 2002, **23**, 3937–3942.
- 119 N. Katayama, H. Kato, Y. Taguchi, A. Tanaka and M. Umeda, *Int. J. Mol. Sci.*, 2014, **15**, 14026–14043.
- 120 M. E. Klontzas, S. Reakasame, R. Silva, J. C. F. Morais, S. Vernardis, R. J. MacFarlane, M. Heliotis, E. Tsiridis, N. Panoskaltzis, A. R. Boccaccini and A. Mantalaris, *Acta Biomater.*, 2019, **88**, 224–240.
- 121 P. W. Kammerer, M. Heller, J. Brieger, M. O. Klein, B. Al-Nawas and M. Gabriel, *Eur. Cell Mater.*, 2011, **21**, 364–372.
- 122 C. Cunha, S. Panseri, O. Villa, D. Silva and F. Gelain, *Int. J. Nanomed.*, 2011, **6**, 943–955.
- 123 S. M. Dallabrida, N. Ismail, J. R. Oberle, B. E. Himes and M. A. Rupnick, *Circ. Res.*, 2005, **96**, e8–24.
- 124 D. Hayoun-Neeman, N. Korover, S. Etzion, R. Ofir, R. G. Lichtenstein and S. Cohen, *Polym. Advan. Technol.*, 2019, **30**, 2493–2505.
- 125 J. Y. Lee, J. E. Choo, Y. S. Choi, J. B. Park, D. S. Min, S. J. Lee, H. K. Rhyu, I. H. Jo, C. P. Chung and Y. J. Park, *Biomaterials*, 2007, **28**, 4257–4267.
- 126 H. J. Lim, M. C. Mosley, Y. Kurosu and L. A. S. Callahan, *Acta Biomater.*, 2017, **56**, 153–160.
- 127 C. E. Cimenci, G. U. Kurtulus, O. S. Caliskan, M. O. Guler and A. B. Tekinay, *Bioconjugate Chem.*, 2019, **30**, 2417–2426.
- 128 H. J. Lim, Z. Khan, T. S. Wilems, X. Lu, T. H. Perera, Y. E. Kurosu, K. T. Ravivarapu, M. C. Mosley and L. A. S. Callahan, *ACS Biomater. Sci. Eng.*, 2017, **3**, 776–781.
- 129 Y. He, C. Mu, X. Shen, Z. Yuan, J. Liu, W. Chen, C. Lin, B. Tao, B. Liu and K. Cai, *Acta Biomater.*, 2018, **80**, 412–424.
- 130 D. Barati, J. D. Walters, S. R. P. Shariati, S. Moeinzadeh and E. Jabbari, *Langmuir*, 2015, **31**, 5130–5140.
- 131 S. Beauvais, O. Drevelle, M. A. Lauzon, A. Daviau and N. Fauchoux, *Acta Biomater.*, 2016, **31**, 241–251.
- 132 Y. Li, Z. Y. Luo, X. Xu, Y. L. Li, S. Q. Zhang, P. Zhou, Y. Sui, M. J. Wu, E. Luo and S. C. Wei, *J. Mater. Chem. B*, 2017, **5**, 7153–7163.
- 133 Y. Yang, Z. Y. Luo and Y. Zhao, *Biopolymers*, 2018, **109**, e23223.
- 134 J. M. Sipes, N. Guo, E. Negre, T. Vogel, H. C. Krutzsch and D. D. Roberts, *J. Cell Biol.*, 1993, **121**, 469–477.
- 135 M. J. Calzada, D. S. Annis, B. Zeng, C. Marcinkiewicz, B. Banas, J. Lawler, D. F. Mosher and D. D. Roberts, *J. Biol. Chem.*, 2004, **279**, 41734–41743.
- 136 V. Castronovo, G. Taraboletti and M. E. Sobel, *J. Biol. Chem.*, 1991, **266**, 20440–20446.
- 137 Z. Zhang, M. J. Gupte, X. Jin and P. X. Ma, *Adv. Funct. Mater.*, 2015, **25**, 350–360.
- 138 I. Bilem, P. Chevallier, L. Plawinski, E. D. Sone, M. C. Durrieu and G. Laroche, *Acta Biomater.*, 2016, **36**, 132–142.
- 139 S. Beauvais, O. Drevelle, M. A. Lauzon, A. Daviau and N. Fauchoux, *Acta Biomater.*, 2016, **31**, 241–251.
- 140 Y. Chen, X. Liu, R. Liu, Y. Gong, M. Wang, Q. Huang, Q. Feng and B. Yu, *Theranostics*, 2017, **7**, 1072–1087.
- 141 I. Bilem, L. Plawinski, P. Chevallier, C. Ayela, E. D. Sone, G. Laroche and M. C. Durrieu, *J. Biomed. Mater. Res. A*, 2018, **106**, 959–970.
- 142 C. M. Rubert Perez, Z. Alvarez, F. Chen, T. Aytun and S. I. Stupp, *ACS Biomater. Sci. Eng.*, 2017, **3**, 2166–2175.
- 143 E. Bergeron, M. E. Marquis, I. Chretien and N. Fauchoux, *J. Mater. Sci. Mater. Med.*, 2007, **18**, 255–263.
- 144 S. H. Park, J. Y. Seo, J. Y. Park, Y. B. Ji, K. Kim, H. S. Choi, S. Choi, J. H. Kim, B. H. Min and M. S. Kim, *NPG Asia Mater.*, 2019, **11**, 30.
- 145 N. Huettner, T. R. Dargaville and A. Forget, *Trends Biotechnol.*, 2018, **36**, 372–383.
- 146 C. M. M. Motta, K. J. Endres, C. Wesdemiotis, R. K. Willits and M. L. Becker, *Biomaterials*, 2019, **218**, 119335.
- 147 R. O. Hynes, *Cell*, 2002, **110**, 673–687.
- 148 B. Nieuwenhuis, B. Haenzi, M. R. Andrews, J. Verhaagen and J. W. Fawcett, *Biol. Rev. Camb. Philos. Soc.*, 2018, **93**, 1339–1362.
- 149 H. Hamidi, M. Pietila and J. Ivaska, *Br. J. Cancer*, 2016, **115**, 1017–1023.
- 150 C. Y. Jiang, X. M. Zeng, B. Xue, D. Campbell, Y. L. Wang, H. F. Sun, Y. M. Xu and X. J. Wen, *Exp. Cell Res.*, 2019, **380**, 90–99.
- 151 R. S. E. D'Souza, M. H. Ginsberg and E. F. Plow, *Trends Biochem. Sci.*, 1991, **16**, 246–250.
- 152 A. Kumar and A. Srivastava, *Nat. Protoc.*, 2010, **5**, 1737–1747.
- 153 L. A. Flanagan, L. M. Rebaza, S. Derzic, P. H. Schwartz and E. S. Monuki, *J. Neurosci. Res.*, 2006, **83**, 845–856.
- 154 C. C. Tate, D. A. Shear, M. C. Tate, D. R. Archer, D. G. Stein and M. C. LaPlaca, *J. Tissue Eng. Regener. Med.*, 2009, **3**, 208–217.
- 155 W. Y. Tjong and H. H. Lin, *Biochem. Biophys. Res. Commun.*, 2019, **520**, 243–249.
- 156 D. Fujii, K. Takase, A. Takagi, K. Kamino and Y. Hirano, *Int. J. Mol. Sci.*, 2021, **22**, 1240.



- 157 Q. Liu, S. Zheng, K. Ye, J. He, Y. Shen, S. Cui, J. Huang, Y. Gu and J. Ding, *Biomaterials*, 2020, **263**, 120327.
- 158 S. A. Maynard, A. Gelmi, S. C. Skaalure, I. J. Pence, C. Lee-Reeves, J. E. Sero, T. E. Whittaker and M. M. Stevens, *ACS Nano*, 2020, **14**, 17321–17332.
- 159 Y. Deng, X. Zhang, Y. Zhao, S. Liang, A. Xu, X. Gao, F. Deng, J. Fang and S. Wei, *Carbohydr. Polym.*, 2014, **101**, 36–39.
- 160 M. Wang, Y. Deng, P. Zhou, Z. Luo, Q. Li, B. Xie, X. Zhang, T. Chen, D. Pei, Z. Tang and S. Wei, *ACS Appl. Mater. Interfaces*, 2015, **7**, 4560–4572.
- 161 Y. M. Chen, L. H. Chen, M. P. Li, H. F. Li, A. Higuchi, S. S. Kumar, Q. D. Ling, A. A. Alarfaj, M. A. Munusamy, Y. Chang, G. Benelli, K. Murugan and A. Umezawa, *Sci. Rep.*, 2017, **7**, 45146.
- 162 Y. Deng, Y. Y. Yang and S. C. Wei, *Biomacromolecules*, 2017, **18**, 587–598.
- 163 Y. Deng, S. C. Wei, L. Yang, W. Z. Yang, M. S. Dargusch and Z. G. Chen, *Adv. Funct. Mater.*, 2018, **28**, 1705546.
- 164 A. Higuchi, S. H. Kao, Q. D. Ling, Y. M. Chen, H. F. Li, A. A. Alarfaj, M. A. Munusamy, K. Murugan, S. C. Chang, H. C. Lee, S. T. Hsu, S. S. Kumar and A. Umezawa, *Sci. Rep.*, 2015, **5**, 18136.
- 165 E. H. Nguyen, M. R. Zanotelli, M. P. Schwartz and W. L. Murphy, *Biomaterials*, 2014, **35**, 2149–2161.
- 166 S. Ali, J. E. Saik, D. J. Gould, M. E. Dickinson and J. L. West, *BioRes. Open Access*, 2013, **2**, 241–249.
- 167 S. J. Bidarra, C. C. Barrias, K. B. Fonseca, M. A. Barbosa, R. A. Soares and P. L. Granja, *Biomaterials*, 2011, **32**, 7897–7904.
- 168 W. U. Park, G. B. Yeon, M. S. Yu, H. G. Goo, S. H. Hwang, D. Na and D. S. Kim, *Biology*, 2021, **10**, 1254.
- 169 K. Sefah, D. Shangguan, X. L. Xiong, M. B. O'Donoghue and W. H. Tan, *Nat. Protocols*, 2010, **5**, 1169–1185.
- 170 L. Li, J. Wan, X. Wen, Q. Guo, H. Jiang, J. Wang, Y. Ren and K. Wang, *Anal. Chem.*, 2021, **93**, 7369–7377.
- 171 S. Saito, *Anal. Sci.*, 2021, **37**, 17–26.
- 172 A. Higuchi, Y. D. Siao, S. T. Yang, P. V. Hsieh, H. Fukushima, Y. Chang, R. C. Ruaan and W. Y. Chen, *Anal. Chem.*, 2008, **80**, 6580–6586.
- 173 K. M. Hennessy, B. E. Pollot, W. C. Clem, M. C. Phipps, A. A. Sawyer, B. K. Culpepper and S. L. Bellis, *Biomaterials*, 2009, **30**, 1898–1909.
- 174 A. A. Sawyer, K. M. Hennessy and S. L. Bellis, *Biomaterials*, 2005, **26**, 1467–1475.
- 175 A. T. Truong, K. Hamada, Y. Yamada, H. Guo, Y. Kikkawa, C. T. Okamoto, J. A. MacKay and M. Nomizu, *FASEB J.*, 2020, **34**, 6729–6740.
- 176 S. Lee, D. S. Lee and J. H. Jang, *Exp. Ther. Med.*, 2021, **21**, 166.
- 177 J. S. Lee, J. S. Lee and W. L. Murphy, *Acta Biomater.*, 2010, **6**, 21–28.
- 178 A. A. Sawyer, D. M. Weeks, S. S. Kelpke, M. S. McCracken and S. L. Bellis, *Biomaterials*, 2005, **26**, 7046–7056.
- 179 P. Y. Lin, S. H. Hung, Y. C. Yang, L. C. Liao, Y. C. Hsieh, H. J. Yen, H. E. Lu, M. S. Lee, I. M. Chu and S. M. Hwang, *Stem Cells Dev.*, 2014, **23**, 372–379.
- 180 E. J. Lee, K. Ahmad, S. Pathak, S. Lee, M. H. Baig, J. H. Jeong, K. O. Doh, D. M. Lee and I. Choi, *Inter. J. Mol. Sci.*, 2021, **22**, 3042.
- 181 S. Raman, G. Srinivasan, N. Brookhouser, T. Nguyen, T. Henson, D. Morgan, J. Cutts and D. A. Brafman, *ACS Biomater. Sci. Eng.*, 2020, **6**, 3477–3490.
- 182 H. W. Kim, K. Yang, W. J. Jeong, S. J. Choi, J. S. Lee, A. N. Cho, G. E. Chang, E. Cheong, S. W. Cho and Y. B. Lim, *ACS Appl. Mater. Interfaces*, 2016, **8**, 26470–26481.
- 183 Y. Vida, D. Collado, F. Najera, S. Claros, J. Becerra, J. A. Andrades and E. Perez-Inestrosa, *RSC Adv.*, 2016, **6**, 49839–49844.
- 184 L. Oliver-Cervello, H. Martin-Gomez, L. Reyes, F. Nouredine, E. Ada Cavalcanti-Adam, M. P. Ginebra and C. Mas-Moruno, *Adv. Healthcare Mater.*, 2021, **10**, e2001757.
- 185 P. Tatray, B. Sagi, A. Szigeti, A. Szepesi, I. Szabo, S. Bosze, Z. Kristof, K. Marko, G. Szakacs, I. Urban, G. Mezo, F. Uher and K. Nemet, *J. Mater. Sci.: Mater. Med.*, 2013, **24**, 479–488.
- 186 C. Chen, H. Li, X. D. Kong, S. M. Zhang and I. S. Lee, *Inter. J. Nanomed.*, 2015, **10**, 283–295.
- 187 B. Dorgau, M. Felemban, G. Hilgen, M. Kiening, D. Zerti, N. C. Hunt, M. Doherty, P. Whitfield, D. Hallam, K. White, Y. Ding, N. Krasnogor, J. Al-Aama, H. Z. Asfour, E. Sernagor and M. Lako, *Biomaterials*, 2019, **199**, 63–75.
- 188 A. Higuchi, Q. D. Ling, S. T. Hsu and A. Umezawa, *Chem. Rev.*, 2012, **112**, 4507–4540.
- 189 F. Mittag, E. M. Falkenberg, A. Janczyk, M. Gotze, T. Felka, W. K. Aicher and T. Kluba, *Orthop. Rev.*, 2012, **4**, e36.
- 190 H. M. Akhri and P. L. Teoh, *Biosci. Rep.*, 2020, **40**, BSR20201325.
- 191 L. Oliveros Anerillas, P. J. Kingham, M. J. Lammi, M. Wiberg and P. Kelk, *Int. J. Mol. Sci.*, 2021, **22**, 13594.
- 192 E. Mazzoni, C. Mazziotta, M. R. Iaquina, C. Lanzillotti, F. Fortini, A. D'Agostino, L. Trevisiol, R. Nocini, G. Barbanti-Brodano, A. Mescola, A. Alessandrini, M. Tognon and F. Martini, *Front. Cell Dev. Biol.*, 2020, **8**, 610570.
- 193 U. Goyal and M. Ta, *Stem Cell Res. Ther.*, 2020, **11**, 181.
- 194 D. Wang, Y. Wang, H. Liu, C. Tong, Q. Ying, A. Sachinidis, L. Li and L. Peng, *J. Cell. Mol. Med.*, 2019, **23**, 3629–3640.
- 195 R. M. Salasnyk, W. A. Williams, A. Boskey, A. Batorsky and G. E. Plopper, *J. Biomed. Biotech.*, 2004, **2004**, 24–34.
- 196 Y. Kang, A. I. Georgiou, R. J. MacFarlane, M. E. Klontzas, M. Heliotis, E. Tsiroidis and A. Mantalaris, *J. Tissue Eng. Regen. Med.*, 2017, **11**, 1929–1940.
- 197 T. C. Sung, J. S. Yang, C. C. Yeh, Y. C. Liu, Y. P. Jiang, M. W. Lu, Q. D. Ling, S. S. Kumar, Y. Chang, A. Umezawa, H. Chen and A. Higuchi, *Biomaterials*, 2019, **221**, 119411.
- 198 Z. Yang, X. Zhao, R. Hao, Q. Tu, X. Tian, Y. Xiao, K. Xiong, M. Wang, Y. Feng, N. Huang and G. Pan, *Proc. Natl. Acad. Sci. U. S. A.*, 2020, **117**, 16127–16137.
- 199 L. Petrone, A. Kumar, C. N. Sutanto, N. J. Patil, S. Kannan, A. Palaniappan, S. Amini, B. Zappone, C. Verma and A. Miserez, *Nat. Commun.*, 2015, **6**, 8737.

- 200 T. Priemel, R. Palia, M. Babych, C. J. Thibodeaux, S. Bourgault and M. J. Harrington, *Proc. Natl. Acad. Sci. U. S. A.*, 2020, **117**, 7613–7621.
- 201 E. Ko, K. Yang, J. Shin and S. W. Cho, *Biomacromolecules*, 2013, **14**, 3202–3213.
- 202 E. W. Danner, Y. Kan, M. U. Hammer, J. N. Israelachvili and J. H. Waite, *Biochemistry*, 2012, **51**, 6511–6518.
- 203 K. Q. Ye, D. H. Liu, H. Z. Kuang, J. Y. Cai, W. M. Chen, B. B. Sun, L. G. Xia, B. Fang, Y. Morsi and X. M. Mo, *J. Colloid Interf. Sci.*, 2019, **534**, 625–636.
- 204 G. F. Gao, T. Yonezawa, K. Hubbell, G. H. Dai and X. F. Cui, *Biotechnol. J.*, 2015, **10**, 1568–1577.
- 205 H. J. Lee, C. Yu, T. Chansakul, N. S. Hwang, S. Varghese, S. M. Yu and J. H. Elisseeff, *Tissue Eng. Pt A*, 2008, **14**, 1843–1851.
- 206 L. Y. Chen, Y. Chang, J. S. Shiao, Q. D. Ling, Y. Chang, Y. H. Chen, D. C. Chen, S. T. Hsu, H. H. C. Lee and A. Higuchi, *Acta Biomater.*, 2012, **8**, 1749–1758.
- 207 A. Higuchi, L. Y. Chen, J. S. Shiao, Q. D. Ling, Y. A. Ko, Y. Chang, Y. Chang, J. T. Bing and S. T. Hsu, *Curr. Nanosci.*, 2011, **7**, 908–914.
- 208 A. Higuchi, S. T. Yang, P. T. Li, M. Tamai, Y. Tagawa, Y. Chang, Y. Chang, Q. D. Ling and S. T. Hsu, *J. Membrane Sci.*, 2010, **351**, 104–111.
- 209 S. S. Kumar, J. H. Hsiao, Q. D. Ling, I. Dulinska-Molak, G. Chen, Y. Chang, Y. Chang, Y. H. Chen, D. C. Chen, S. T. Hsu and A. Higuchi, *Biomaterials*, 2013, **34**, 7632–7644.
- 210 M. Becker, S. Lorenz, D. Strand, C. F. Vahl and M. Gabriel, *Scientific World J.*, 2013, **2013**, 616535.
- 211 J. Dhillon, S. A. Young, S. E. Sherman, G. I. Bell, B. G. Amsden, D. A. Hess and L. E. Flynn, *J. Biomed. Mater. Res., Part A*, 2019, **107**, 571–585.
- 212 E. C. Qin, S. T. Ahmed, P. Sehgal, V. H. Vu, H. Kong and D. E. Leckband, *Biomaterials*, 2020, **239**, 119846.
- 213 T. W. Chung, D. Z. Liu, S. Y. Wang and S. S. Wang, *Biomaterials*, 2003, **24**, 4655–4661.
- 214 R. Fraioli, K. Dashnyam, J. H. Kim, R. A. Perez, H. W. Kim, J. Gil, M. P. Ginebra, J. M. Manero and C. Mas-Moruno, *Acta Biomater.*, 2016, **43**, 269–281.
- 215 J. E. Frith, R. J. Mills and J. J. Cooper-White, *J. Cell Sci.*, 2012, **125**, 317–327.
- 216 N. A. Silva, M. J. Cooke, R. Y. Tam, N. Sousa, A. J. Salgado, R. L. Reis and M. S. Shoichet, *Biomaterials*, 2012, **33**, 6345–6354.
- 217 J. Yan, X. L. Lu, X. C. Zhu, X. K. Hu, L. L. Wang, J. Qian, F. M. Zhang and M. Liu, *Inter. J. Nanomed.*, 2020, **15**, 497–511.
- 218 O. Koniev and A. Wagner, *Chem. Soc. Rev.*, 2015, **44**, 5495–5551.
- 219 N. J. Smith, K. Rohlfing, L. A. Sawicki, P. M. Kharkar, S. J. Boyd, A. M. Kloxin and J. M. Fox, *Org. Biomol. Chem.*, 2018, **16**, 2164–2169.
- 220 M. C. Hacker and H. A. Nawaz, *Int. J. Mol. Sci.*, 2015, **16**, 27677–27706.
- 221 R. Y. Tam, M. J. Cooke and M. S. Shoichet, *J. Mater. Chem.*, 2012, **22**, 19402–19411.
- 222 T. Hayakawa, M. Yoshinari and K. Nemoto, *J. Biomed. Mater. Res. A*, 2003, **67**, 684–688.
- 223 T. V. Chirila, T. Minamisawa, I. Keen and K. Shiba, *Macromol. Biosci.*, 2009, **9**, 959–967.
- 224 J. T. Koepsel, P. T. Brown, S. G. Loveland, W. J. Li and W. L. Murphy, *J. Mater. Chem.*, 2012, **22**, 19474–19481.
- 225 J. R. Klim, L. Li, P. J. Wrighton, M. S. Piekarczyk and L. L. Kiessling, *Nat. Methods*, 2010, **7**, 989–994.
- 226 K. A. Kilian and M. Mrksich, *Angew. Chem., Int. Ed.*, 2012, **51**, 4891–4895.
- 227 G. A. Hudalla and W. L. Murphy, *Langmuir*, 2010, **26**, 6449–6456.
- 228 P. D. Tatman, E. G. Muhonen, S. T. Wickers, A. O. Gee, E. S. Kim and D. H. Kim, *Biomater. Sci.*, 2016, **4**, 543–554.
- 229 T. H. Kim, E. B. Ko, S. J. Kim and J. W. Choi, *J. Biomed. Nanotechnol.*, 2013, **9**, 307–311.
- 230 E. S. Kang, H. Kim, Y. Han, Y. W. Cho, H. Son, Z. T. Luo and T. H. Kim, *Colloids Surf., B*, 2021, **204**, 111807.
- 231 D. Salah, F. S. Moghanm, M. Arshad, A. A. Alanazi, S. Latif, M. I. El-Gammal, E. M. Shima and S. Elsayed, *Diagnostics*, 2021, **11**, 1196.
- 232 Y. Deng, X. Zhang, X. Zhao, Q. Li, Z. Ye, Z. Li, Y. Liu, Y. Zhou, H. Ma, G. Pan, D. Pei, J. Fang and S. Wei, *Acta Biomater.*, 2013, **9**, 8840–8850.
- 233 P. Gentile, C. Ghione, C. Tonda-Turo and D. M. Kalaskar, *RSC Adv.*, 2015, **5**, 80039–80047.
- 234 X. J. Zhou, W. Feng, K. X. Qiu, L. Chen, W. Z. Wang, W. Nie, X. M. Mo and C. L. He, *ACS Appl. Mater. Interfaces*, 2015, **7**, 15777–15789.
- 235 L. D. Kong, C. S. Alves, W. X. Hou, J. R. Qiu, H. Mohwald, H. Tomas and X. Y. Shi, *ACS Appl. Mater. Interfaces*, 2015, **7**, 4833–4843.
- 236 S. Patntirapong, W. Janvikul, T. Theerathanagorn and W. Singhatanadgit, *J. Biomater. Appl.*, 2017, **31**, 859–870.
- 237 R. Mobasser, L. L. Tian, M. Soleiman, S. Ramakrishna and H. Naderi-Manesh, *Mater. Sci. Eng., C*, 2018, **84**, 80–89.
- 238 G. Onak, M. Sen, N. Horzum, U. K. Ercan, Z. B. Yarali, B. Garipcan and O. Karaman, *Sci. Rep.*, 2018, **8**, 17620.
- 239 T. Richardson, C. Wiegand, F. Adisa, K. Ravikumar, J. Candiello, P. Kumta and I. Banerjee, *Acta Biomater.*, 2020, **113**, 228–239.
- 240 M. Wang, T. Yang, Q. Bao, M. Yang and C. Mao, *ACS Appl. Mater. Interfaces*, 2022, **14**, 350–360.
- 241 C. A. Simmons, E. Alsberg, S. Hsiong, W. J. Kim and D. J. Mooney, *Bone*, 2004, **35**, 562–569.
- 242 S. X. Hsiong, T. Boonthekul, N. Huebsch and D. J. Mooney, *Tissue Eng., Part A*, 2009, **15**, 263–272.
- 243 T. Re'em, O. Tsur-Gang and S. Cohen, *Biomaterials*, 2010, **31**, 6746–6755.
- 244 C. M. Madl, M. Mehta, G. N. Duda, S. C. Heilshorn and D. J. Mooney, *Biomacromolecules*, 2014, **15**, 445–455.
- 245 M. Mehta, C. M. Madl, S. Lee, G. N. Duda and D. J. Mooney, *J. Biomed. Mater. Res., Part A*, 2015, **103**, 3516–3525.
- 246 Z. Y. Luo, S. Q. Zhang, J. J. Pan, R. Shi, H. Liu, Y. L. Lyu, X. Han, Y. Li, Y. Yang, Z. X. Xu, Y. Sui, E. Luo, Y. Y. Zhang and S. C. Wei, *Biomaterials*, 2018, **163**, 25–42.

- 247 Y. Ren, H. Zhang, W. J. Qin, B. Du, L. R. Liu and J. Yang, *Mater. Sci. Eng., C*, 2020, **108**, 110276.
- 248 Y. P. Long, L. S. Yan, H. L. Dai, D. Yang, X. P. Wu, X. Z. Dong, K. Liu, W. Y. Wei and Y. Z. Chen, *Mater. Sci. Eng., C*, 2020, **116**, 111258.
- 249 B. Ananthanarayanan, L. Little, D. V. Schaffer, K. E. Healy and M. Tirrell, *Biomaterials*, 2010, **31**, 8706–8715.
- 250 Y. Hirano, Y. Kando, T. Hayashi, K. Goto and A. Nakajima, *J. Biomed. Mater. Res.*, 1991, **25**, 1523–1534.
- 251 W. Huang, X. Wu, X. Gao, Y. Yu, H. Lei, Z. Zhu, Y. Shi, Y. Chen, M. Qin, W. Wang and Y. Cao, *Nat. Chem.*, 2019, **11**, 310–319.
- 252 Y. Oz, A. Barras, R. Sanyal, R. Boukherroub, S. Szunerits and A. Sanyal, *ACS Appl. Mater. Interfaces*, 2017, **9**, 34194–34203.
- 253 M. D. Perretti, L. A. Perez-Marquez, R. Garcia-Rodriguez and R. Carrillo, *J. Org. Chem.*, 2019, **84**, 840–850.
- 254 J. Pupkaite, J. Rosenquist, J. Hilborn and A. Samanta, *Biomacromolecules*, 2019, **20**, 3475–3484.
- 255 S. Q. Liu, Q. A. Tian, L. Wang, J. L. Hedrick, J. H. P. Hui, Y. Y. Yang and P. L. R. Ee, *Macromol. Rapid Commun.*, 2010, **31**, 1148–1154.
- 256 C. N. Salinas and K. S. Anseth, *J. Tissue Eng. Regener. Med.*, 2008, **2**, 296–304.
- 257 Z. P. Zhang, M. J. Gupte, X. B. Jin and P. X. Ma, *Adv. Funct. Mater.*, 2015, **25**, 350–360.
- 258 M. Song, H. Jang, J. Lee, J. H. Kim, S. H. Kim, K. Sun and Y. Park, *Biomaterials*, 2014, **35**, 2436–2445.
- 259 J. H. Park, G. J. Gillispie, J. S. Copus, W. B. Zhang, A. Atala, J. J. Yoo, P. C. Yelick and S. J. Lee, *Biofabrication*, 2020, **12**, 035029.
- 260 R. Nunez-Toldra, P. Dosta, S. Montori, V. Ramos, M. Atari and S. Borros, *Acta Biomater.*, 2017, **53**, 152–164.
- 261 I. Bilem, L. Plawinski, P. Chevallier, C. Ayela, E. D. Sone, G. Laroche and M. C. Durrieu, *J. Biomed. Mater. Res., Part A*, 2018, **106**, 959–970.
- 262 I. Bilem, P. Chevallier, L. Plawinski, E. D. Sone, M. C. Durrieu and G. Laroche, *Acta Biomater.*, 2016, **36**, 132–142.
- 263 J. Park, J. M. Heo, S. Seong, J. Noh and J. M. Kim, *Nat. Commun.*, 2021, **12**, 4207.
- 264 M. M. Xu, X. Y. You, Y. Z. Zhang, Y. Lu, K. Tan, L. Yang and Q. Cai, *J. Am. Chem. Soc.*, 2021, **143**, 8993–9001.
- 265 Q. Li, D. M. Xing, L. Ma and C. Y. Gao, *Mater. Sci. Eng., C*, 2017, **73**, 562–568.
- 266 J. L. Ratcliffe, M. Walker, A. M. Eissa, S. R. Du, S. A. Przyborski, A. L. Laslett and N. R. Cameron, *J. Polym. Sci. Polym. Chem.*, 2019, **57**, 1974–1981.
- 267 F. Y. Cao, W. N. Yin, J. X. Fan, L. Tao, S. Y. Qin, R. X. Zhuo and X. Z. Zhang, *ACS Appl. Mater. Interfaces*, 2015, **7**, 6698–6705.
- 268 A. N. Sohi, H. Naderi-Manesh, M. Soleimani, E. R. Yasaghi, H. K. Manjili, S. Tavaddod and S. Nojehdehi, *Mater. Sci. Eng., C*, 2018, **93**, 157–169.
- 269 P. T. Nyffeler, C. H. Liang, K. M. Koeller and C. H. Wong, *J. Am. Chem. Soc.*, 2002, **124**, 10773–10778.
- 270 J. Dvorakova, J. Trousil, B. Podhorska, Z. Miksovska, O. Janouskova and V. Proks, *Biomacromolecules*, 2021, **22**, 1417–1431.
- 271 B. El-Zaatari, A. C. Tibbits, Y. Yan and C. J. Kloxin, *ACS Macro Lett.*, 2019, **8**, 795–799.
- 272 H. Wu, H. Li, R. T. Kwok, E. Zhao, J. Z. Sun, A. Qin and B. Z. Tang, *Sci. Rep.*, 2014, **4**, 5107.
- 273 Y. Rong, Z. Zhang, C. L. He and X. S. Chen, *Sci. China: Chem.*, 2020, **63**, 1100–1111.
- 274 J. Dommerholt, O. van Rooijen, A. Borrmann, C. F. Guerra, F. M. Bickelhaupt and F. L. van Delft, *Nat. Commun.*, 2014, **5**, 5378.
- 275 J. Dommerholt, F. Rutjes and F. L. van Delft, *Top. Curr. Chem.*, 2016, **374**, 16.
- 276 N. E. Mbua, J. Guo, M. A. Wolfert, R. Steet and G. J. Boons, *ChemBioChem*, 2011, **12**, 1912–1921.
- 277 L. A. Callahan, S. Xie, I. A. Barker, J. Zheng, D. H. Reneker, A. P. Dove and M. L. Becker, *Biomaterials*, 2013, **34**, 9089–9095.
- 278 J. E. Hein and V. V. Fokin, *Chem. Soc. Rev.*, 2010, **39**, 1302–1315.
- 279 M. Ghollasi and D. Poormoghadam, *J. Biomed. Mater. Res. A*, 2022, **110**, 672–683.
- 280 C. C. Yu, Y. W. Chen, P. Y. Yeh, Y. S. Hsiao, W. T. Lin, C. W. Kuo, D. Y. Chueh, Y. W. You, J. J. Shyue, Y. C. Chang and P. Chen, *J. Nanobiotechnol.*, 2019, **17**, 31.
- 281 M. Mahmoodinia Maymand, H. R. Soleimanpour-Lichaei, A. Ardeshirylajimi, M. Soleimani, S. E. Enderami, S. Nojehdehi, F. Behjati and M. Kabir Salmani, *Artif. Cells, Nanomed., Biotechnol.*, 2018, **46**, 853–860.
- 282 J. A. Rowley and D. J. Mooney, *J. Biomed. Mater. Res.*, 2002, **60**, 217–223.
- 283 B. H. Chueh, Y. Zheng, Y. S. Torisawa, A. Y. Hsiao, C. X. Ge, S. Hsiong, N. Huebsch, R. Franceschi, D. J. Mooney and S. Takayama, *Biomed. Microdevices*, 2010, **12**, 145–151.
- 284 A. Zamuner, P. Brun, M. Scorzeto, G. Sica, I. Castagliuolo and M. Dettin, *Bioact. Mater.*, 2017, **2**, 121–130.
- 285 M. Ebara, M. Yamato, T. Aoyagi, A. Kikuchi, K. Sakai and T. Okano, *Biomacromolecules*, 2004, **5**, 505–510.
- 286 C. Mo, L. Xiang and Y. Chen, *Macromol. Rapid Commun.*, 2021, **42**, e2100025.
- 287 L. R. M. Lima, E. L. L. Ramos, M. F. S. Silva, F. O. S. Ribeiro, J. S. Sousa, C. Pessoa, D. A. Silva, J. P. A. Feitosa, H. C. B. Paula and R. C. M. de Paula, *Int. J. Biol. Macromol.*, 2021, **166**, 144–154.
- 288 M. J. M. Carneiro, C. B. A. Paula, I. S. Ribeiro, L. R. M. de Lima, F. O. S. Ribeiro, D. A. Silva, G. S. Araujo, J. D. B. Marinho Filho, A. J. Araujo, R. S. Freire, J. P. A. Feitosa and R. C. M. de Paula, *Int. J. Biol. Macromol.*, 2021, **185**, 390–402.
- 289 X. Mou, H. Zhang, H. Qiu, W. Zhang, Y. Wang, K. Xiong, N. Huang, H. A. Santos and Z. Yang, *Research*, 2022, **2022**, 9780879.
- 290 W. Wei, J. Yu, M. A. Gebbie, Y. Tan, N. R. Martinez Rodriguez, J. N. Israelachvili and J. H. Waite, *Langmuir*, 2015, **31**, 1105–1112.
- 291 P. J. Wrighton, J. R. Klim, B. A. Hernandez, C. H. Koonce, T. J. Kamp and L. L. Kiessling, *Proc. Natl. Acad. Sci. U. S. A.*, 2014, **111**, 18126–18131.
- 292 M. J. Kim, B. Lee, K. Yang, J. Park, S. Jeon, S. H. Um, D. I. Kim, S. G. Im and S. W. Cho, *Biomaterials*, 2013, **34**, 7236–7246.